RATE DETERMINATION OF THE CO_2* CHEMILUMINESCENCE REACTION

$$CO + O + M = CO_2^* + M$$

A Thesis

by

MADELEINE MARISSA KOPP

Submitted to the Office of Graduate Studies of
Texas A&M University
in partial fulfillment of the requirements for the degree of

MASTER OF SCIENCE

Approved by:

Chair of Committee,	Eric L. Petersen
Committee Members,	Rodney D. W. Bowersox
	David A. Staack
Head of Department,	Jerald A. Caton

December 2012

Major Subject: Mechanical Engineering

ABSTRACT

The use of chemiluminescence measurements to monitor a range of combustion processes has been a popular area of study due to their reliable and cost-effective nature. Electronically excited carbon dioxide (CO_2*) is known for its broadband emission, and its detection can lead to valuable information; however, due to its broadband characteristics, CO_2* is difficult to isolate experimentally, and the chemical kinetics of this species is not well known. Although numerous works have monitored CO_2* chemiluminescence, a full kinetic scheme for the species has yet to be developed.

A series of shock-tube experiments was performed in H_2-N_2O-CO mixtures highly diluted in argon at conditions where emission from CO_2* could be isolated and monitored. These results were used to evaluate the kinetics of CO_2*, in particular, the main CO_2* formation reaction, $CO + O + M \rightleftarrows CO_2^* + M$ (R1). Based on collision theory, the quenching chemistry of CO_2* was determined for eleven common collision partners. The final mechanism developed for CO_2* consisted of 14 reactions and 13 species. The rate for R1 was determined based on low-pressure experiments performed in two different H_2-N_2O-CO-Ar mixtures.

Final mechanism predictions were compared with the experimental results at low and high pressures, with good agreement seen at both conditions. Peak CO_2* trends with temperature as well as overall CO_2* species time histories were both monitored. Comparisons were also made with previous experiments in methane-oxygen mixtures, where there was slight over-prediction of CO_2* experimental trends by the mechanism.

Experimental results and mechanism predictions were also compared with past literature rates for CO_2*, with good agreement for peak CO_2* trends, and slight discrepancies in overall CO_2* species time histories. Overall, the ability of the CO_2* mechanism developed in this work to reproduce a range of experimental trends represents an improvement over existing models.

ACKNOWLEDGMENTS

I would like to first and foremost thank my advisor and committee chair, Dr. Petersen, for his exceptional guidance throughout my research experience both as an undergraduate and graduate student. Thanks also go out to my committee members, Dr. Bowersox and Dr. Staack, for their help and support in serving on my committee.

I also owe gratitude to my co-workers, who have helped tremendously in making this work possible. Special thanks go out to Dr. Olivier Mathieu for his help in running experiments, as well as to Marissa Brower, for her work in the initial stages of the project. Finally, I would like to acknowledge my family, whose moral support has been a tremendous source of encouragement and perseverance.

NOMENCLATURE

[X]	Molar concentration of species X
ν	Fundamental frequency
k	Reaction rate coefficient
A	Pre-exponential factor
n	Temperature exponent
E_a	Activation energy
$\bar{R}$	Universal gas constant
N	Number of moles
H_R	Heat of reaction
$\bar{h}_f^o$	Heat of formation at 298 K and 1 atm
ΔE	Energy difference between ground and excited state
h	Planck's constant
c	Speed of light
λ	Wavelength of chemiluminescence transition
N_A	Avogadro's number
c_p	Constant pressure specific heat
H^o	Enthalpy
S^o	Entropy
ΔH_f	Enthalpy of formation
Z	Collision frequency

σ_{AB}	Mean collision diameter of molecules A and B
k_b	Boltzmann constant
μ_{AB}	Reduced mass of molecules A and B

TABLE OF CONTENTS

Page

LIST OF FIGURES

Page

LIST OF TABLES

Page

CHAPTER I

INTRODUCTION

Chemiluminescence has proven to be a significant diagnostic tool for combustion health monitoring. Its relative simplicity and non-intrusive nature make it ideal for a variety of applications such as heat release sensing [1-6], equivalence ratio detection [5-8], and fuel consumption rate monitoring [4].

Chemiluminescence describes the process in which a molecule transitions from an excited state to its ground state, causing a release of energy in the form of light. Common excited state species that have been studied are OH* [6, 9-27], CH* [6, 8, 9, 21, 28-30], NH* [21, 28, 30], and NO* [29, 31], among others. A crucial aspect in the study of chemiluminescence is the ability of chemical kinetics mechanisms to predict measured trends. The chemistry of OH* and CH*(A) is the most well-known, and their detection is easily accessible due to their sharp emission features near 307 nm and 431 nm, respectively, as shown in Figure 1. However, the chemistry of other species such as CO_2*, HCO*, and CH_2O*, also shown in Figure 1, is less well-known due in part to the fact that their emission features are more broadband in nature, so they are difficult to isolate experimentally.

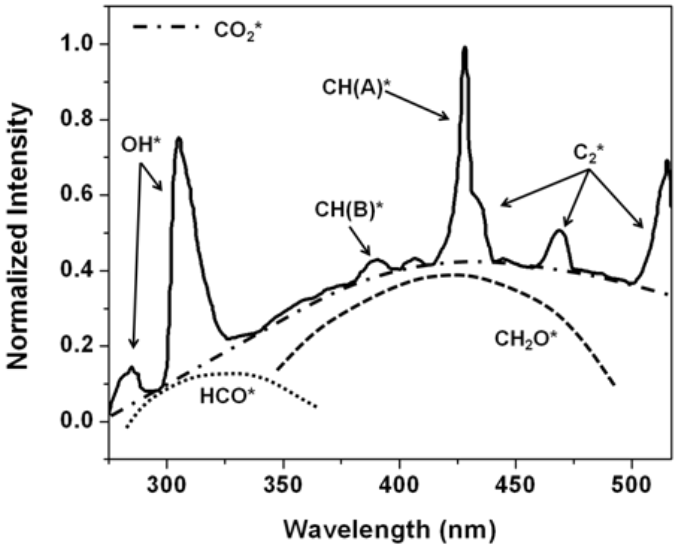

Figure 1. Recreation of a portion of the chemiluminescence spectrum showing the broadband background of the chemiluminescence from CO_2*, HCO*, and CH_2O*, based on work from [4, 5, 8, 32, 33]**.**

Much of the broadband background emission in hydrocarbon flames has been attributed to emission from CO_2* [1, 4, 5, 33-47], but the various proposed kinetics mechanisms for CO_2* [4, 8, 35, 36, 40, 48-59] are not in complete consensus. It has been identified by Broida and Gaydon [60] and Laidler and Shuler [59] that the main reaction that goes to forming CO_2* is

$$CO + O + M \rightleftarrows CO_2^* + M \qquad \text{R1}$$

However, the rate for this reaction is still up for debate [40, 48, 61], and there is discrepancy as to the overall order of this reaction as well [48, 53, 57, 59, 62]. Although several works have made measurements of CO_2* chemiluminescence [1-5, 8, 9, 34-38,

40, 41, 43, 45, 46, 48, 51-54, 56, 58, 63-72], most have been geared toward determining the rate of the CO_2 radiative recombination [38, 42, 50-54, 58, 60, 63, 68]:

$$CO + O \rightleftarrows CO_2 + h\nu$$

Due to the lack of consensus on CO_2* chemiluminescence chemistry in general, the goal of this study was to formulate a complete kinetics scheme for the formation and depletion of CO_2* and determine the rate of the title reaction, R1, using a combination of fundamental kinetics theory as well as a fitting scheme to experimental data. This thesis provides an overview of the existing contributing works available in the literature as well as a brief background and review of kinetics theory in Chapter II. In Chapter III, the experimental apparatus and chemical kinetics modeling are described, and the experimental conditions of the study are presented. Chapter III also includes the rate-determining process for R1. The results are presented in Chapter IV along with an uncertainty analysis on the proposed kinetics scheme. Comparisons with alternate kinetic schemes and a high-pressure excursion are also presented in Chapter IV. Finally, Chapter V provides conclusions and identifies future avenues of research for continuation of this work.

CHAPTER II

LITERATURE REVIEW AND BACKGROUND

Literature Review

Chemiluminescence from electronically excited CO_2 (herein denoted at CO_2*) consists of a broad continuum that can extend from below 300 nm to above 600 nm [1, 4, 33-43, 59] along with discrete CO flame bands [35, 36, 41, 42, 48, 59, 60, 68, 70]. While the continuum is more prominent at high temperatures (above 1000 K) [35, 36], the flame bands are known to be favored at lower temperatures [35, 36, 42, 70]. The blue radiation observed in carbon monoxide flames is also said to come from CO_2* emission [35, 38, 42, 50, 60].

Despite the extensive amount of work addressing CO_2* chemiluminescence, its full chemical kinetics mechanism is still under debate. Because of its broadband nature, CO_2* is difficult to isolate experimentally, so verification of the kinetics mechanism is challenging. Rather than using a full kinetics mechanism for CO_2*, many studies have relied on the fact that CO_2* chemiluminescence is proportional to the product of the concentrations of carbon monoxide and atomic oxygen [9, 35, 36, 38, 43, 47, 48, 52, 57, 58, 62, 63, 68, 73].

Studies of CO_2* chemiluminescence have dated back to as early as the 1950's. In 1951, Laidler and Shuler [59] studied gas-phase elementary reactions involving excited electronic states, in which CO_2* emission was addressed. They attributed the carbon

dioxide continuum to the process $CO+O \rightarrow CO_2^* \rightarrow CO_2+h\nu$ and identified R1 as a likely source for CO_2^* in the carbon monoxide flame. Gordon and Knipe [49] investigated the kinetics of carbon monoxide and oxygen in 1955, and Kaskan [43] explored the source of the continuum in CO-H_2-air flames in 1959, concluding that the continuum accounts for approximately 95% of the radiation and suggesting that the light intensity should be proportional to the product of [CO] and [O].

A number of additional works on CO_2^* were published in the 1960's. In 1962, Clyne and Thrush [35] measured intensities of the chemiluminescent emission from CO_2^* and NO_2^* at low temperatures (200 – 300 K) and found that CO_2^* emission occurs from below 300 nm to above 500 nm, with peak intensity around 400 nm. The kinetics of CO_2^* were detailed in a later work by Clyne and Thrush [48] in 1963. Information on the carbon monoxide flame bands was presented by Dixon [70] in 1963, with an extensive discussion on the electronic structure and molecular configuration of CO_2 in its ground and excited states. Davies [36] studied carbon dioxide dissociation at high temperatures (6,000 – 11,000 K) behind reflected shock waves in 1965 and discussed the nature of the excited state of CO_2 at these conditions. In another shock-tube study by Myers [52] in 1967, a rate constant for the radiative recombination of carbon monoxide and oxygen was determined by recording emission intensity at six spectral intervals between 250 and 800 nm.

The 1970's and 80's saw a continued interest in the chemistry of CO_2^*, and a few works stand out. The exponential growth rate of CO_2^* chemiluminescence was measured in shock-heated H_2-CO-O_2-Ar mixtures by Schott [56] in 1973, and in another

work by Schott et al. [38] in 1974, oxygen-atom yields were determined by monitoring CO_2* emission and using the relation that intensity is proportional to the concentration product of [CO] and [O], as was done by Jachimowski in 1974 [68]. Gaydon [42] identified CO_2* as the source of carbon monoxide flame bands and provided an extensive discussion on CO_2* emission and chemical kinetics in a 1976 text.

Several works dedicated to CO_2* chemiluminescence measurements were conducted in the 1980's. In 1981, Pravilov and Smirnova [54] made room-temperature CO_2* chemiluminescence measurements in a small, homogeneous reactor, and in 1985, Slack and Grillo [58] made spectral measurements of CO_2* chemiluminescence between 260 and 700 nm at high temperatures (1300 – 2700 K) in shock-heated H_2-O_2-CO-CO_2-Ar mixtures. A study in 1986 was conducted by Malerich and Scanlon [51] in which measurements from a homogeneous reactor were compared to theoretical calculations of the radiative recombination of CO and O.

Only a few studies in the 1990's were conducted concerning CO_2* chemiluminescence. One of the more significant was from Samaniego et al. [4] in 1995, in which it was determined that CO_2* accounts for more than 95% of chemiluminescence in CH_4-O_2-N_2 flames over the spectral interval of 340 to 600 nm. In this study, it was determined that CO_2* chemiluminescence correlated with various flame characteristics, such as fuel consumption rate, heat release rate, and H-atom concentration.

In 2002, Kim et al. [2] made detailed spectral measurements in SI, HCCI, and SCCI engines from various excited state species and determined that CO_2* emission

correlated well with heat release. Bessler et al. [34] conducted a study in 2003 concerning carbon dioxide laser-induced fluorescence (LIF) in high-pressure methane flames, in which the broad continuum (200 to 450 nm) was attributed to CO_2*. Shortly thereafter, in 2004, Lee et al. [37] conducted UV planar laser-induced fluorescence (PLIF) measurements of CO_2* in laminar methane-air flames at pressures up to 20 atm. They found that CO_2 detection is highly temperature dependent and could potentially be used to infer temperature in practical combustion devices.

In the last five years, several works regarding CO_2* chemiluminescence have been noteworthy. In 2007 and 2008, Nori and Seitzman [5, 8] made OH*, CH*, and CO_2* chemiluminescence measurements in syngas and methane flames and observed good agreement with model predictions. CO_2* measurements were made by Schuermans et al. [46] in 2010 in thermo-acoustic modeling of a gas turbine, and in 2011, Gupta et al. [1] studied the use of CO_2* chemiluminescence in natural gas-fired reciprocating engines, attributing over 90% of the integrated emission signal over the visible spectrum to CO_2*. They also pointed out that the CO_2* mechanism is in need of refinement, thus facilitating the need for the current study.

In a 2011 work, Vesel et al. [41] studied dissociation of CO_2 molecules in a microwave plasma at high temperatures (up to 2500 K) and observed a high continuum, attributing it to CO_2* chemiluminescence. Kopp et al. [72] formulated a first-generation kinetics mechanism for CO_2* chemiluminescence in 2012 and compared model predictions to shock-tube experimental data at low and elevated pressures. This recent work by the present author brought about the need for further chemical kinetics

refinement. A number of other recent works concerning CO_2* were conducted recently [45, 64-67, 69], but these concern measurements in the infrared (IR) range, which is associated with vibrational rather than electronic transitions.

Kinetics Theory

CO_2 Reaction Kinetics*

Although a number of works have addressed possible mechanisms for the formation and depletion of CO_2* [4, 8, 35, 36, 40, 42, 48-59], there is no complete consensus as to the full reaction set. One of the most fundamental theories governing CO_2* formation is the proportional relationship between CO_2* emission intensity and the concentration product of atomic oxygen and carbon dioxide, shown by Equation 1 [35, 36, 38, 43, 47, 48, 52, 57, 58, 62, 63, 68, 73].

$$CO_2^* \propto [CO][O] \tag{1}$$

This relationship has been shown to fairly accurately predict peak-magnitude temperature dependence at low and elevated pressures, as seen in the work of Kopp et al [72], but it still does not provide a reaction rate that can be incorporated into chemical kinetics mechanisms, which is of the form

$$k = AT^n \exp\left(\frac{-E_a}{\bar{R}T}\right) \tag{2}$$

where k is the rate coefficient, A is the pre-exponential factor, n is the temperature exponent, E_a is the activation energy, and $\bar{R}$ is the universal gas constant.

The main reaction that goes to forming CO_2* has been shown by Laidler and Schuler [59] and Broida and Gaydon [60] to be R1, although its rate has not been directly measured. It is the goal of this study to provide a rate for this reaction that accurately predicts measured CO_2* trends. However, to use experimental data to systematically tailor this rate, the supporting CO_2* chemistry must be determined. A first-generation mechanism for CO_2* was recently established by Kopp et al. [72], the formulation of which is briefly described here.

First, thermodynamic calculations were made to determine the reactions that were energetic enough to produce CO_2*. This step was done by calculating the heat of reaction, H_R, for every reaction in the ground-state chemical kinetics mechanism that contained CO_2 as a participant. The heat of reaction was calculated using Equation 3:

$$H_R = \sum_i N_i \left(\bar{h}^o_{f,i}\right)_{products} - \sum_j N_j \left(\bar{h}^o_{f,j}\right)_{reactants} \quad (3)$$

where N is the number of moles, $\bar{h}^o_f$ is the heat of formation at the reference state (298 K, 1 atm), and the subscripts i and j denote each product and reactant species, respectively.

Next, the energy difference, ΔE, between the ground-state (CO_2) and the excited state (CO_2*), was calculated using Equation 4,

$$\Delta E = \frac{hc}{\lambda} N_A \quad (4)$$

where h is Planck's constant (6.626×10^{-34} J-s), c is the speed of light (3×10^8 m/s), λ is the wavelength of the chemiluminescence transition, and N_A is Avogadro's Number (6.022×10^{23} mole^{-1}). An average value of 495 nm was used for the wavelength of CO_2*

chemiluminescence transition, assuming CO_2* is present at wavelengths between 340 and 650 nm. The reactions in which H_R was greater than ΔE were then identified as being energetic enough to produce CO_2*. These are denoted by R1 and R2 in Table 1.

Table 1. Reaction mechanism for CO_2*. Units are cal, cm, mole, sec, K.

#	Reaction	A	n	E_a	Source
R1	$CO + O + M \rightleftharpoons CO_2^* + M$	4.00×10^{14}	0	2384	This Work
	Efficiency Factors: H_2 2, H_2O 12, CO 1.75, CO_2 3.6, Ar 0.7, He 0.7				NUIG Ground-state
R2	$HCO + O \rightleftharpoons CO_2^* + H$	3.00×10^{13}	0	0	NUIG Ground-state
R3	$CO_2^* + Ar \rightleftharpoons CO_2 + Ar$	8.42×10^{12}	0.5	0	This Work
R4	$CO_2^* + H_2O \rightleftharpoons CO_2 + H_2O$	8.34×10^{12}	0.5	0	This Work
R5	$CO_2^* + CO_2 \rightleftharpoons CO_2 + CO_2$	9.12×10^{12}	0.5	0	This Work
R6	$CO_2^* + CO \rightleftharpoons CO_2 + CO$	9.69×10^{12}	0.5	0	This Work
R7	$CO_2^* + H \rightleftharpoons CO_2 + H$	3.07×10^{13}	0.5	0	This Work
R8	$CO_2^* + H_2 \rightleftharpoons CO_2 + H_2$	2.27×10^{13}	0.5	0	This Work
R9	$CO_2^* + O_2 \rightleftharpoons CO_2 + O_2$	8.77×10^{12}	0.5	0	This Work
R10	$CO_2^* + O \rightleftharpoons CO_2 + O$	9.82×10^{12}	0.5	0	This Work
R11	$CO_2^* + OH \rightleftharpoons CO_2 + OH$	9.87×10^{12}	0.5	0	This Work
R12	$CO_2^* + CH_4 \rightleftharpoons CO_2 + CH_4$	1.19×10^{13}	0.5	0	This Work
R13	$CO_2^* + N_2 \rightleftharpoons CO_2 + N_2$	9.96×10^{12}	0.5	0	This Work
R14	$CO_2^* \rightleftharpoons CO_2 + h\nu$	1.00×10^{6}	0	0	This Work

The next step was to formulate Arrhenius rate coefficients (A, n, and E_a) to use for these reactions in the chemical kinetics mechanism, as shown in Equation 2. These were taken to be the same as their respective ground-state reactions. In addition to R1 and R2, CO_2* consumption reactions were added, denoted by R3 – R13 in Table 1,

which included quenching from 11 common quenching partners. The rate coefficients for these reactions were calculated based on the hard-sphere collision theory, as discussed in the following section. The last reaction in the mechanism, R14, is the spontaneous emission reaction, and its rate was estimated to be 1×10^6 sec^{-1}. Since a direct measurement of this rate could not be found, it was taken to be similar to those that have been measured for NO* (4.55×10^6 sec^{-1}), OH* (1.45×10^6 sec^{-1}), and CH* (1.85×10^6 sec^{-1}) [21], which all agree with Gaydon's observation that radiative lifetimes for transitions in the visible and ultra-violet range from 10^{-8} to 10^{-6} sec [42].

Finally, new thermodynamic data for CO_2* were developed. These data are most commonly in the form of the three following polynomial fits:

$$\frac{c_{p,k}^o}{\bar{R}} = a_{1k} + a_{2k}T_k + a_{3k}T_k^2 + a_{4k}T_k^3 + a_{5k}T_k^4 \tag{5}$$

$$\frac{H_k^o}{\bar{R}T_k} = a_{1k} + \frac{a_{2k}}{2}T_k + \frac{a_{3k}}{3}T_k^2 + \frac{a_{4k}}{4}T_k^3 + \frac{a_{5k}}{5}T_k^4 + \frac{a_{6k}}{T_k} \tag{6}$$

$$\frac{S_k^o}{\bar{R}} = a_{1k}\ln(T_k) + a_{2k}T_k + \frac{a_{3k}}{2}T_k^2 + \frac{a_{4k}}{3}T_k^3 + \frac{a_{5k}}{4}T_k^4 + a_{7k} \tag{7}$$

where the seven coefficients, $a_{1\text{-}7}$, for each species, k, are used to characterize the three thermodynamic properties of that species: c_p (constant pressure specific heat), H^o (enthalpy), and S^o (entropy). Since these coefficients are specified for two temperature ranges, 300 – 1000 K and 1000 – 5000 K, there are a total of 14 thermodynamic coefficients for each species.

To simplify calculations, it was assumed that c_p and S^o for CO_2* were the same as the ground state values. A similar assumption is typically made for the other, more well known chemiluminescent species OH* and CH*. This assumption left a_6 as the

only unknown coefficient for both temperature ranges. This coefficient was determined by first calculating the enthalpy of formation of CO_2* ($\Delta H_{f,CO_2^*}$) by adding ΔE to the enthalpy of ground state CO_2. Then for each of the two temperature ranges, a_6 was calculated by iteratively changing the coefficient in Equation 6 until $H^o/\bar{R}T$ matched $\Delta H_{f,CO_2^*}/\bar{R}T$. A temperature of 300 K was used for the low-temperature range calculations, and 1000 K was used for the high-temperature range calculations. The resulting thermodynamic data can be found in the Appendix, where a_6 was calculated as -3.74×10^2 for the low-temperature range and -1.03×10^3 for the high-temperature range.

Quenching Theory

Quenching is the process in which an electronically excited species is returned to its ground state due to a collision with another molecule [59, 74], represented by the general expression,

$$A^* + B \rightarrow A + B \tag{8}$$

where *A* is the molecule being quenched, and *B* is the colliding molecule. For a bimolecular reaction such as this, the rate coefficient is given by

$$k = Ze^{-E_a/\bar{R}T} \tag{9}$$

where *Z* is the frequency of collisions per volume per unit concentration. From basic collision theory, the collision frequency is given by

$$Z = \sigma_{AB}^2 \left[\frac{8\pi k_b T}{\mu_{AB}}\right]^{1/2} \tag{10}$$

where σ_{AB} is the mean collision diameter of molecules A and B, k_b is the Boltzmann constant (1.381×10^{-23} J K^{-1}), and μ_{AB} is the reduced mass of the collision pair [59].

A basic interpretation of the proposed theory is to assume $E_a = 0$, in which case the rate coefficient is equal to the collision frequency, and the remaining terms in Equation 2 reduce to n = ½ and

$$A = N_A \sigma_{AB}^2 \left[\frac{8\pi k_b}{\mu_{AB}}\right]^{1/2} \tag{11}$$

In this way, the rate expressions for the quenching reactions for CO_2* were determined for 11 common collision partners, denoted by R3 – R13 in Table 1. The molecular parameters necessary for these calculations are listed in Table 2.

Table 2. Molecular parameters used in the hard-sphere calculations for CO_2* quenching reactions, taken from Turns [75].

Species	Collision Diameter (m)	Molecular Weight (g/mol)
CO_2	3.941×10^{-10}	44.01
Ar	3.542×10^{-10}	39.948
H_2O	2.641×10^{-10}	18.016
CO_2	3.941×10^{-10}	44.011
CO	3.690×10^{-10}	28.01
H_2	2.827×10^{-10}	2.016
O_2	3.467×10^{-10}	31.999
OH	3.147×10^{-10}	17.007
H	2.708×10^{-10}	1.008
O	3.050×10^{-10}	16
CH_4	3.758×10^{-10}	16.043
N_2	3.798×10^{-10}	28.013

CHAPTER III

EXPERIMENTAL SETUP AND MODELING

Shock-Tube Experimental Setup

Experiments were performed in the high-pressure, stainless-steel shock-tube facility described in detail by Aul [76]. It consists of a 4.93-m long driver section and a 4.72-m driven section, separated by a polycarbonate or aluminum diaphragm. When the driver section is pressurized by an inert gas (helium, in this case), the diaphragm bursts, sending a shock wave to propagate through the driven section of the tube, which is filled to a lower pressure with the gas mixture of interest before the start of each test. The reflection of this shock wave off the endwall of the shock tube creates the high-temperature and -pressure conditions necessary for these measurements.

The temperature and pressure behind the reflected shock wave were determined using standard 1-D shock relations. At five intervals along the driven section of the shock tube, PCB-P113A pressure transducers mounted flush with the inner surface of the tube signal the passage of the shock wave, which determines the incident-shock velocity recorded by four Fluke PM 6666 time-interval counters. The final shock velocity is then extrapolated to the endwall location. The uncertainty in temperature using this method is less than 10 K [77].

The mixtures in this study were manometrically prepared in a stainless steel mixing tank with a perforated stinger along the center of the tank to facilitate rapid,

turbulent mixing. High-purity gases (H_2, Ar – 99.999%, CO – 99.9%, N_2O – 99.5%) were used to prepare the test mixtures. Dilution levels were maintained at 95.95 % Ar to minimize subsequent heat release and pressure rise due to the combustion process, so that temperature and pressure would remain constant at the test conditions to allow for more-accurate chemical kinetics modeling. Details on the mixtures used in this study are provided in a later section.

Chemiluminescence light emission was collected through a Sapphire window 1.6 cm from the endwall at a sidewall location. The light from the window passed through a 1-mm slit and focused onto a Hamamatsu 1P21 photomultiplier tube (PMT) after passing through an optical filter housed just outside in a custom-made enclosure. To capture CO_2* chemiluminescence, an optical filter centered at 415 nm was used, which lies within the broadband spectrum of CO_2*, as shown in Figure 1. In a study by Kopp et al. [72], it was confirmed that at these experimental conditions, the emission through either a 458-nm or a 415-nm filter gave the same results, so the 415-nm filter was chosen for this study, which gave better signal-to-noise ratios than the 458-nm filter.

Chemical Kinetics Modeling

All kinetics calculations were performed using the homogeneous batch reactor routine in the Chemkin software collection [78], assuming constant volume and constant internal energy. The H_2-O_2 chemistry from the National University of Ireland, Galway (NUIG) formed the baseline mechanism [79, 80], which was fortified by NO_x chemistry

from the work of Mathieu et al. [81]. The full mechanism, including the CO_2* chemistry, can be found in the Appendix.

Experimental Conditions

The experimental conditions for this study were chosen so that CO_2* chemiluminescence could be isolated from other emitting species and so that the rate for R1 could be as isolated as possible. Two mixtures were chosen for these purposes, the first of which was taken from the work of Dean et al. [82] who used shock-heated mixtures of H_2-N_2O-CO-Ar to measure the rate constant of the reaction $H + N_2O \rightleftarrows N_2 + OH^*$. This mixture was chosen because it exhibited unique characteristics in the various predicted excited-state species time histories, as shown in Figure 2. As seen in Figure 2, the peak concentrations of OH*, CO_2*, and CH_2O* occur at noticeably different times, and the shape of the profiles are clearly discernible from one another, making this mixture an ideal one to isolate a particular species, such as CO_2*.

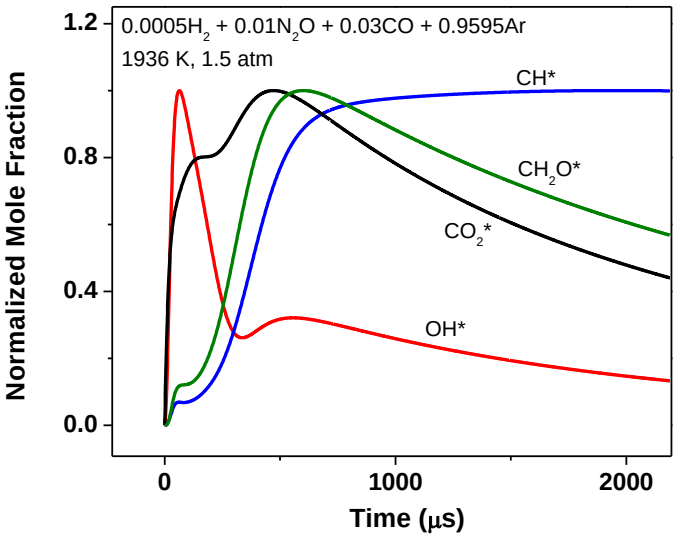

Figure 2. Model predictions for various chemiluminescence species in $0.0005H_2$ + $0.01N_2O$ + 0.03CO + 0.9595Ar at 1936 K and 1.5 atm. Profiles are normalized to peak values.

Another compelling reason to choose this mixture was that the predicted peak magnitudes of the other excited-state hydrocarbon species, CH_2O* and CH*, were around 6 and 10 orders of magnitude less than the peak magnitude of CO_2*, which added confidence that the measured emission from the experiment was primarily from CO_2*, as the emission from the other hydrocarbon species would be too low to detect. All measurements in this mixture, denoted as "Mix 0", were made previously and are presented in the work of Kopp et al. [72].

The second mixture, denoted as "Mix 1", was a derivative of the first one and chosen to facilitate the determination for R1 in the CO_2* reaction mechanism. The mole

fractions of the two mixtures are presented in Table 3, and average experimental conditions are presented in Table 4.

Table 3. Mixture compositions for Mix 0 and Mix 1, in % volume.

	% H_2	% N_2O	% CO	% Ar
Mix 0	0.0005	0.01	0.03	0.9595
Mix 1	0.0005	0.02	0.02	0.9595

Table 4. Experimental conditions for Mix 0 and Mix 1 in terms of average pressures and temperature range.

	Average Pressures (atm)	Temperature Range (K)	Source
Mix 0	1.4, 10.4	1654 - 2202	Kopp et al. (2012)
Mix 1	1.5	1700 - 2222	This Work

Fitting Scheme

The rate for R1 was determined by an iterative process to match the trends exhibited by the experimental data. The main criterion for the fitting was the CO_2* peak magnitude, which was determined from the PMT measurement for each experiment. A typical time history from the PMT measurement is shown in Figure 3, which shows the rise and fall of CO_2* chemiluminescence for an experiment at 1700 K and 1.6 atm in Mix 1.

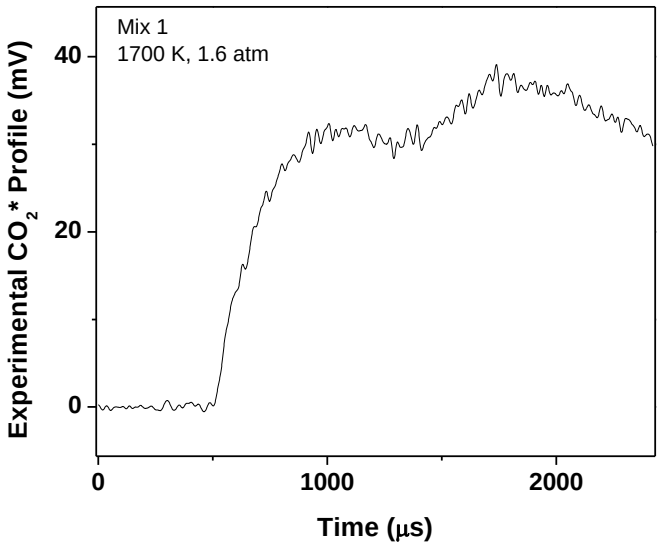

Figure 3. Experimental CO_2* time history showing PMT output in mV as a function of time in microseconds at 1700 K and 1.6 atm in Mix 1.

For each experiment, the CO_2* time history was recorded, and the peak was graphically determined. In most cases, there was a noticeable double feature in the time history, as seen in Figure 3, with a small hump at the beginning, giving rise to the larger peak later on. For the most part, the second hump was higher than the first, so the peak was always taken to be the maximum from the second feature. This assignment was done to provide consistency in data interpretation, even if the first peak was comparable in magnitude to the second. Note that the experimental time histories presented here were graphically smoothed for presentation purposes. The signal-to-noise ratio was usually between 20 and 70.

To compare experimental trends with model predictions, the peaks were normalized to a common value within that experimental set, which was usually the highest-temperature case. This normalization was done because the PMT measurement is not an absolute concentration measurement of the CO_2* species, and there was no calibration available that related PMT output in volts to species concentration. Figure 4 shows a plot of the normalized peaks for experiments in Mix 0. Despite the moderate signal-to-noise ratio in the time histories, the resulting scatter in the data in Figure 4 is small.

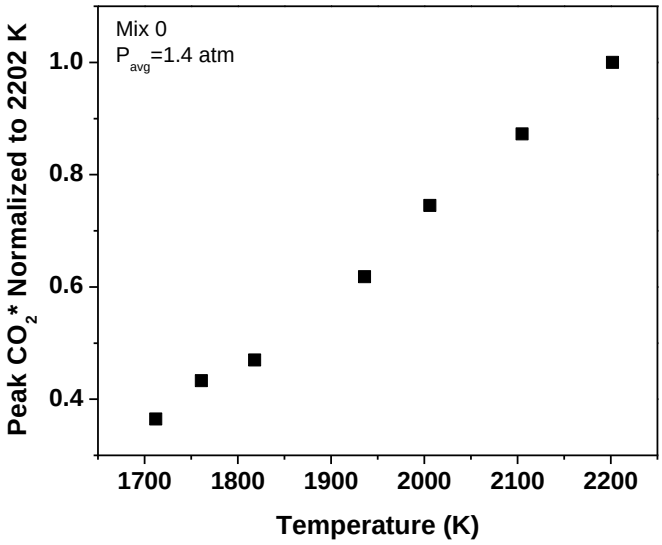

Figure 4. Peak CO_2* normalized to 2202 K for experiments in Mix 0 at an average pressure of 1.4 atm.

As Figure 4 shows, there is a clear temperature dependence of the peak CO_2* magnitude, and this trend was a crucial aspect in determining the rate of R1. For each mixture, the peak magnitude trends of the mechanism were compared with the experimental results. As a starting point, the rate for R1 was taken to be the low-pressure rate from the ground-state reaction,

$$CO + O + M \rightleftarrows CO_2 + M$$

which is a third-order rate and has units of $cm^6/mole^2$-sec. In addition, the ground-state collision frequencies were included (see Table 1), and these were not changed throughout the rate determining process. Figure 5 shows an example of the mechanism predictions using this ground-state rate for R1 (i.e., the original, baseline model).

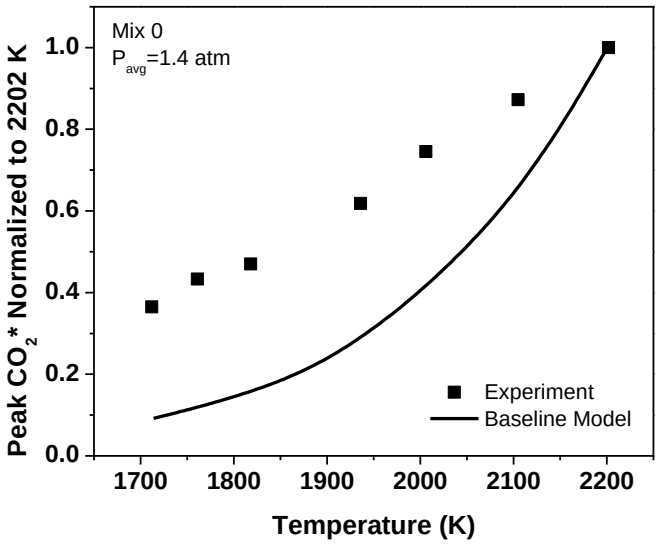

Figure 5. Peak CO_2* mechanism predictions with experimental data from Mix 0 using the ground-state rate for R1.

As Figure 5 shows, the temperature dependence of the CO_2* peak magnitude is highly under-predicted by this baseline mechanism, as was the case for Mix 1 experiments, and to improve these predictions, sensitivity and rate of production analyses were conducted, which indicated which reactions were most sensitive to the formation and depletion of CO_2*. Typical results of these calculations are shown in Figure 6 at an intermediate temperature for Mix 0 and Mix 1.

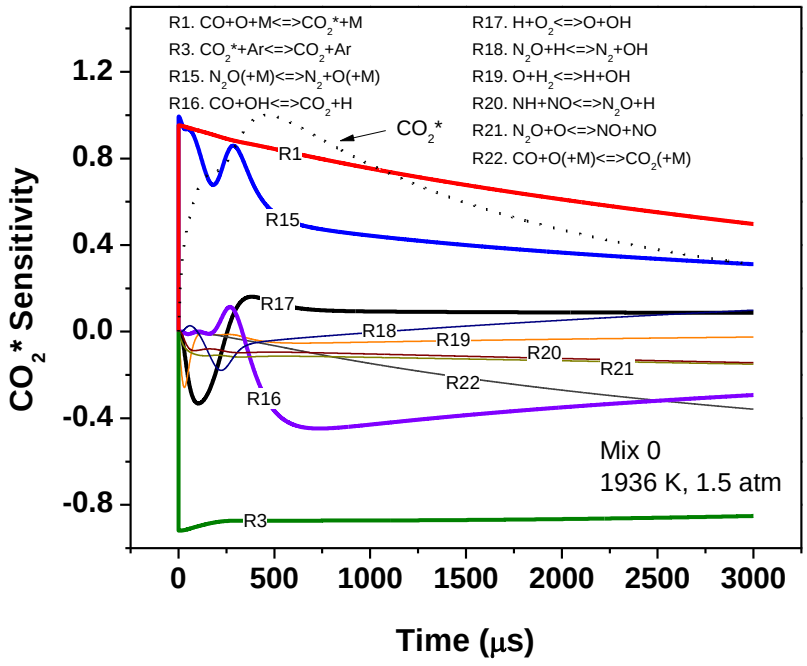

(a)

Figure 6. CO_2* sensitivity and rate of production analysis at 1936 K and 1.5 atm for Mix 0 (a), (c) and Mix 1 (b), (d).

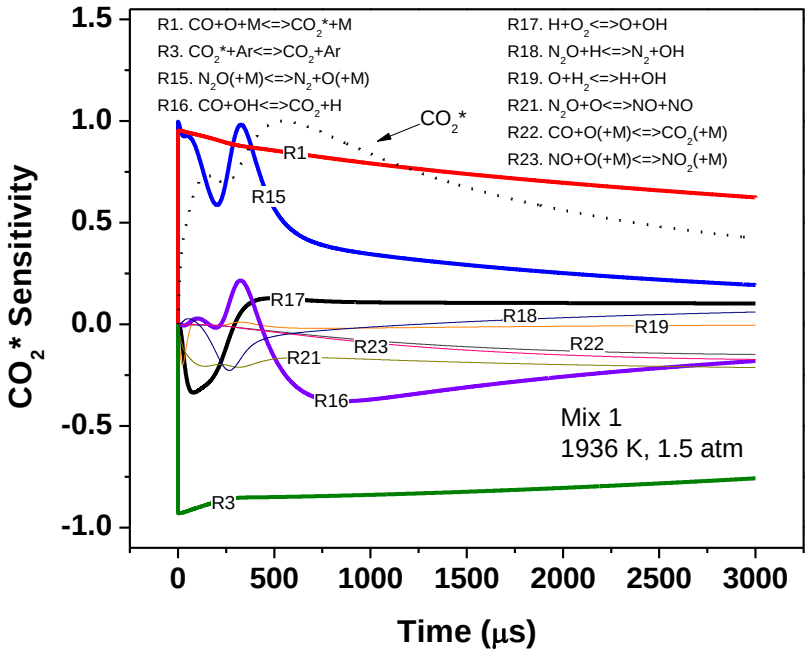

(b)

Figure 6. Continued.

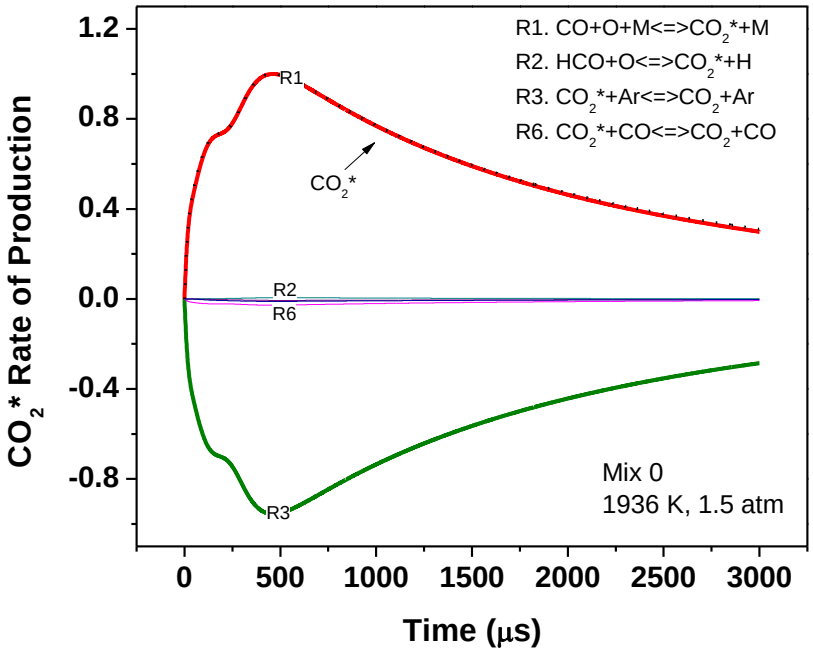

(c)

Figure 6. Continued

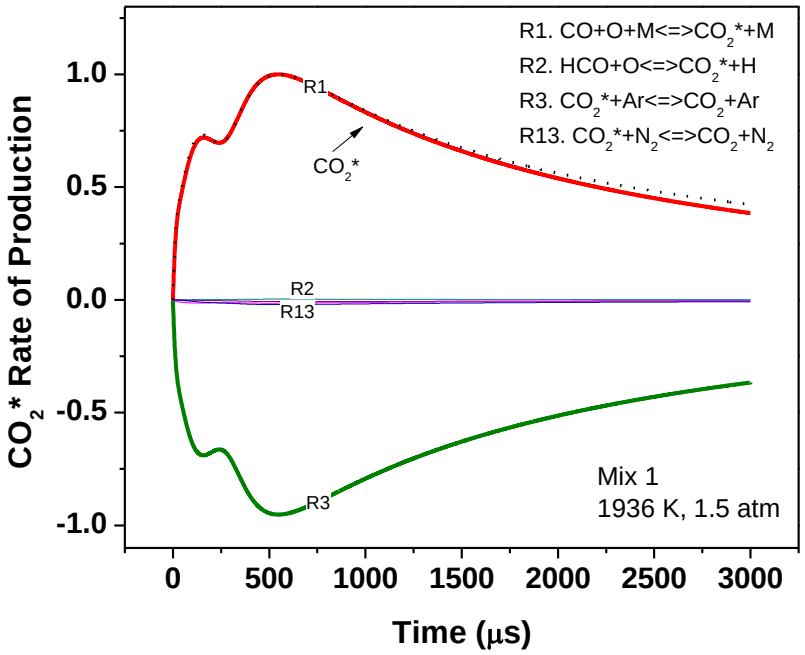

(d)

Figure 6. Continued.

The trends are quite similar for both mixtures in terms of which reactions are most sensitive to CO_2* production and depletion. All results were normalized to a common peak value to allow for direct comparison between the various reactions.

The most important reactions indicated by Figure 6 are as follows:

$$CO + O + M \rightleftarrows CO_2^* + M \qquad \text{R1}$$

$$CO_2^* + Ar \rightleftarrows CO_2 + Ar \qquad \text{R3}$$

$$N_2O(+M) \rightleftarrows N_2 + O(+M) \qquad \text{R15}$$

$$CO + OH \rightleftarrows CO_2 + H \qquad \text{R16}$$

At the time of peak CO_2*, R1 is most sensitive for CO_2* production, while the argon quenching reaction (R3) is almost equally important for removing CO_2*, seen in Figure 6 (a) and (b). A couple of ground-state reactions also stood out as being sensitive for CO_2* production and depletion, even though they don't have CO_2* as either a product or reactant. The pressure-dependent decomposition reaction of N_2O is quite sensitive for CO_2* production, while reaction R16 is sensitive for CO_2* destruction. The rate of production analyses shown in Figure 6 (c) and (d) indicate the reactions that go to forming and depleting CO_2* at these conditions, which are R1 and R3, respectively.

Unfortunately, it was impossible to completely isolate R1 to be the only reaction sensitive to the peak CO_2*. Therefore, the rate of R1 determined in this work was inherently linked to the accuracy of R3, R15, and R16 as well, and uncertainty in R1 due to differences in these rates is presented in Chapter IV.

Since the baseline mechanism under-predicted the peak CO_2* trends, an increase in the rate for R1 was necessary. It was assumed that the current activation energy (2,384 cal/mole) of this reaction was sufficient, which came from the ground-state reaction chemistry. Changing this parameter to fit the peak trends of the experiments greatly reduced the agreement with species time histories. This fixing of the activation energy left the pre-exponential factor, A, as the variable to be determined in this work. This parameter was incrementally increased until the peak trends from the experiments in Mix 0 and Mix 1 were most accurately predicted in both cases. In addition to peak magnitude agreement, time history agreement was also monitored. Based on peak

magnitude and time history agreement, the pre-exponential factor for R1 was determined as 4.0×10^{14} $cm^6/mole^2$-sec. The full Arrhenius rate expression is as follows:

$$k_{R1} = 4.0 \times 10^{14} \exp\left(-2{,}384/\bar{R}T\right)\ cm^6/mole^2 sec$$

where the activation energy has units of cal/mole. Final comparisons with this rate to experimental data are presented in the following chapter.

CHAPTER IV

RESULTS AND DISCUSSION

Temperature Dependence of Peak Magnitude

Table 5 lists the CO_2* peak magnitude determined from each experiment for Mix 0 and Mix 1 that were used to calculate R1.

Table 5. Temperature, pressure, and peak CO_2* signal from the experiments used to determine R1.

Mix 0		
Temperature (K)	**Pressure (atm)**	**CO_2* Signal Peak (mV)**
1712	1.49	49.8
1761	1.47	59.1
1818	1.44	64.1
1936	1.46	84.4
2006	1.41	101.7
2105	1.38	119.1
2202	1.33	136.5
Mix 1		
Temperature (K)	**Pressure (atm)**	**CO_2* Signal Peak (mV)**
1700	1.56	38.2
1730	1.55	38.5
1802	1.54	48.8
1897	1.48	60.5
1911	1.56	64.6
1927	1.47	63.0
2015	1.44	75.4
2108	1.41	86.5
2205	1.42	104.5
2222	1.38	101.7

The data are presented graphically in Figure 7 along with the mechanism predictions using the final rate determined for R1, which was $4.0\times10^{14}\exp(-2{,}384/\bar{R}T)$ $cm^6/mole^2$-sec as mentioned above and summarized in Table 1.

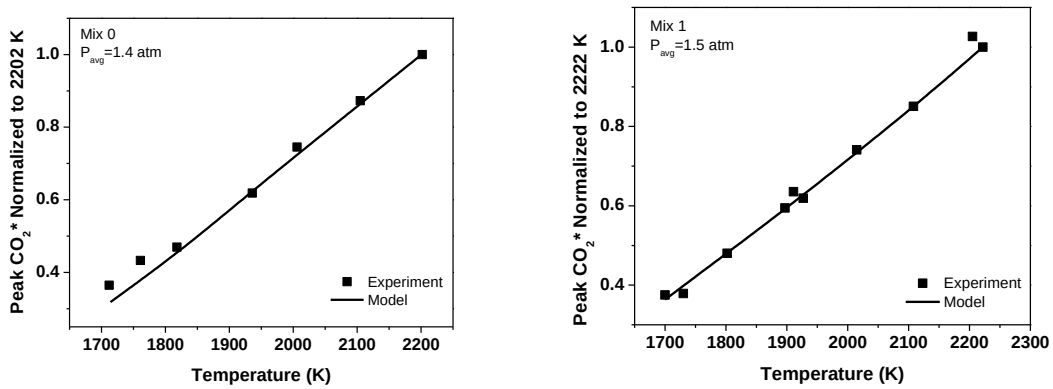

(a) (b)

Figure 7. Normalized peak CO_2* from experiments compared with final mechanism predictions for Mix 0 (a) and Mix 1 (b).

Using this rate for R1 along with the supporting chemistry described in Chapter III, Figure 7 shows that the model very accurately predicts the CO_2* peak magnitude temperature dependence trends in both mixtures. It is shown in a later section that the model also does well at predicting peak CO_2* trends at higher pressures and does a fairly good job at predicting trends in a methane-based mixture.

Species Time Histories

Aside from peak magnitude trends, it was also important to consider overall CO_2* species time histories in determining the rate for R1. Figure 8 shows the final mechanism predictions in comparison with experiments in Mix 0 and Mix 1. Three temperatures are presented to show the evolution of the species time history as temperature is increased. The profiles were normalized to peak values to allow for comparison between model and data. In addition, the profiles predicted by the mechanism were shifted in time to align with the initial rise of CO_2* from the experiment to facilitate comparison of the overall shape of the profiles.

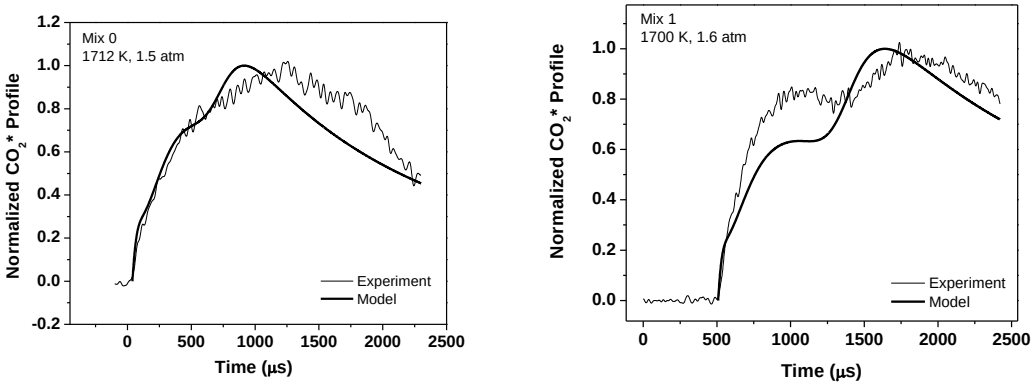

(a) (b)

Figure 8. Normalized CO_2* experimental profiles compared with the final mechanism predictions for low, medium, and high temperature in Mix 0 (a), (c), (e) and Mix 1 (b), (d), (f).

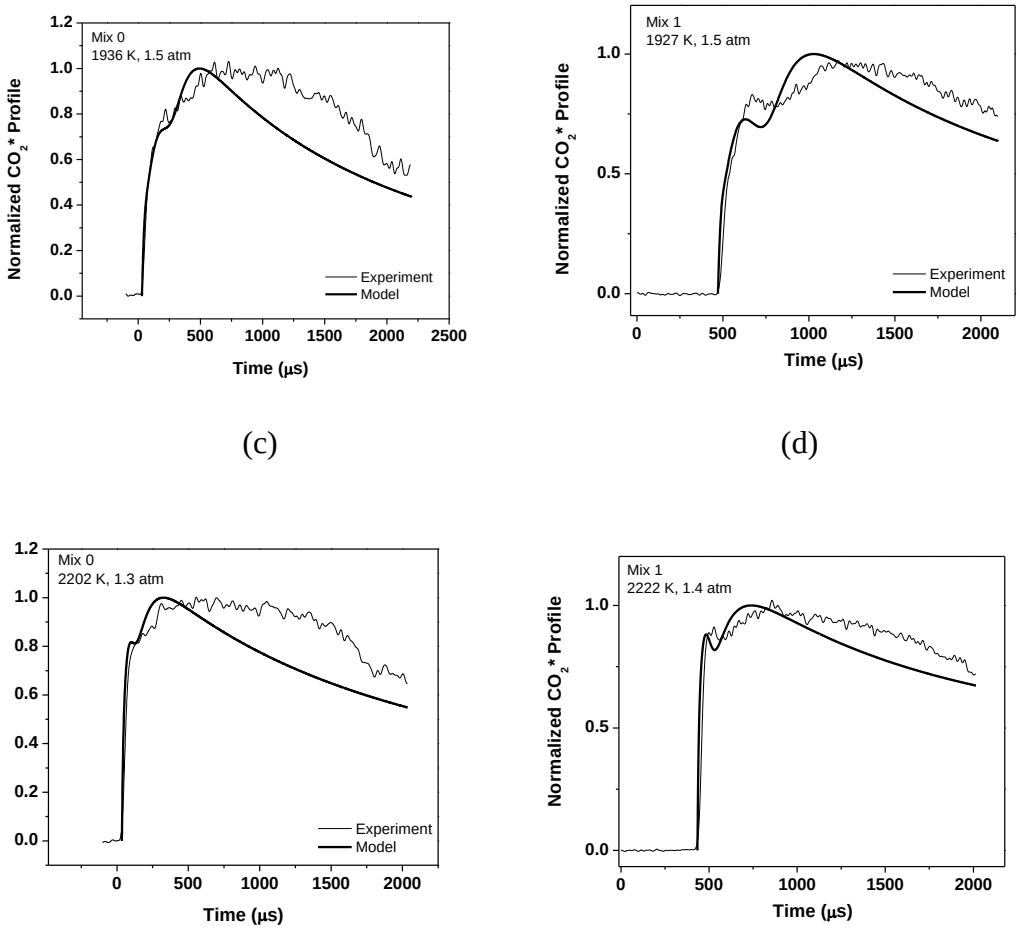

Figure 8. Continued.

The CO_2* experimental profiles in both mixtures exhibited a double feature, with a small, sometimes very subtle incipient hump giving rise to a larger and broader maximum in the profile. The two features are slightly more discernible in Mix 1, with the first hump closer in magnitude to the second. This is a rather unique feature, and the fact that the mechanism picks up on it is quite promising. While the agreement is not

perfect, the small subtleties in the experimental time histories are present in the mechanism predictions, and perhaps agreement could be improved with slight adjustments in the ground-state chemistry.

In Mix 0, the leading edge of the CO_2* experimental profile is fairly accurately modeled by the mechanism at all three temperatures, as seen in Figure 8 (a), (c), and (e). However, the trailing edge is slightly under-predicted by the mechanism, which predicts a faster CO_2* decay than the experiment at these conditions. The trailing edge is better predicted by the mechanism in Mix 1, as seen in Figure 8 (b), (d), and (f), although the incipient rise is slightly under-predicted at the low (b) and moderate (d) temperatures. In most cases, for both mixtures, the mechanism predicts a faster peak than the experiment, but not by much. Changes to the CO_2* chemistry will most likely not change this answer, as the excited-state chemistry mostly governs the peak magnitudes of a species and not the overall shape. The timing of the species is more dependent rather on the ground-state chemistry, which in this case R15 and R16 could have an effect on this parameter, as shown by the sensitivity analyses in Figure 6 (a) and (b).

Uncertainty

Since it was not possible to completely isolate R1 to determine its rate, it was necessary to consider upper and lower bounds on a few of the other reactions that were sensitive in the formation and depletion of CO_2*. The reactions considered in this

uncertainty analysis were R3, R15, and R16, as these were shown in Figure 6 (a) and (b) to be most sensitive for CO_2* formation and consumption.

Figure 9 shows the effect of an increase and decrease of one order of magnitude in the pre-exponential factor of R3, the CO_2* quenching rate by argon.

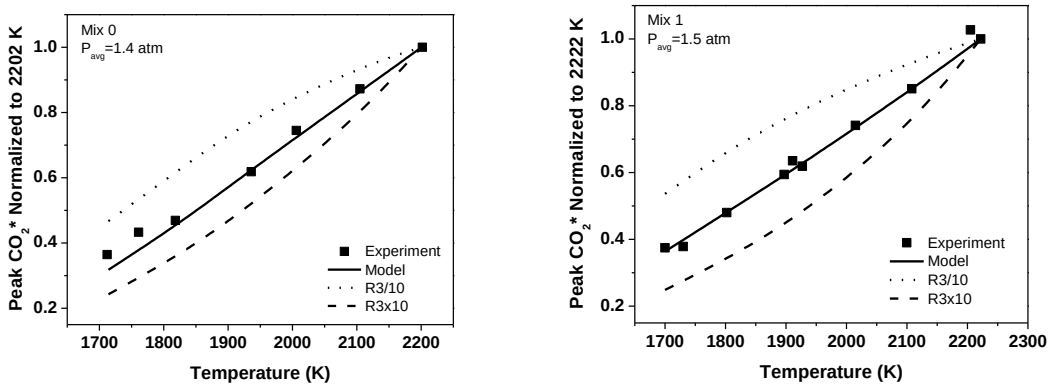

(a) (b)

Figure 9. Effect of changes to $CO_2^* + Ar \rightleftarrows CO_2 + Ar$ **(**R3) on mechanism predictions compared to normalized CO_2* peak trends from experiments in Mix 0 (a) and Mix 1 (b).

As expected, an order of magnitude increase in this rate causes an under-prediction of the peak magnitude trend by about 20% in both mixtures. This result is due to the negative sensitivity of this reaction to the formation of CO_2*, so an increase in this rate would decrease the amount of CO_2* produced. Conversely, an order of magnitude decrease in this rate causes an over-prediction of peak magnitude trends by about 30% in Mix 0 and 25% in Mix 1. It should be noted that this rate has never been measured or validated, and its current value is based on the hard sphere theoretical calculations

presented in Chapter II. In OH* chemistry, a species that has been studied more extensively, quenching by argon has been measured to be up to two orders of magnitude less than theoretical calculations [15, 19]. However, in a study by Holtermann et al. [83], measured quenching by argon of SO_2* was comparable to theoretical calculations, as was quenching by argon of propynal in a study by Thayer and Yardley [84]. Therefore, it was concluded that an order-of-magnitude increase or decrease in this rate (R3) would be sufficient in determining the uncertainty limits in calculations for R1.

The next most important rate in CO_2* formation was R15, which came from the NO_x ground-state chemistry submechanism. Figure 10 shows the effect of an increase in this rate by about five times and a decrease by about 15 times. These upper and lower bounds came from the general consensus of variation in the rate from both theoretical and experimental studies [85]. There is little effect of increasing this rate to its upper limit, as shown by the dotted line in Figure 10. However, decreasing this rate by about 15 times leads to an under-prediction of peak CO_2* by around 20% in Mix 0 and 30% in Mix 1. The higher-percentage difference in Mix 1 is most likely due to the increase of N_2O present in this mixture compared to Mix 0.

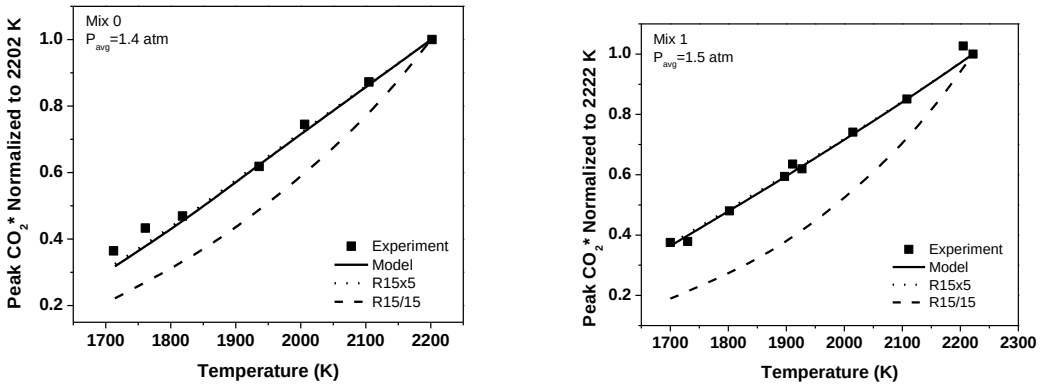

(a) (b)

Figure 10. Effect of changes to $N_2O(+M) \rightleftarrows N_2 + O(+M)$ **(**R15) on mechanism predictions compared to normalized CO_2* peak trends from experiments in Mix 0 (a) and Mix 1 (b).

The last reaction considered in the uncertainty analysis was R16, which displays a negative sensitivity to CO_2* at the time of peak CO_2* formation, as shown by Figure 6 (a) and (b) in Chapter III. The effect of increasing this rate by around three times and decreasing it by around six times is shown in Figure 11. Again, these upper and lower bounds were based on the general variation in this rate from a mass of past theoretical and experimental studies [85].

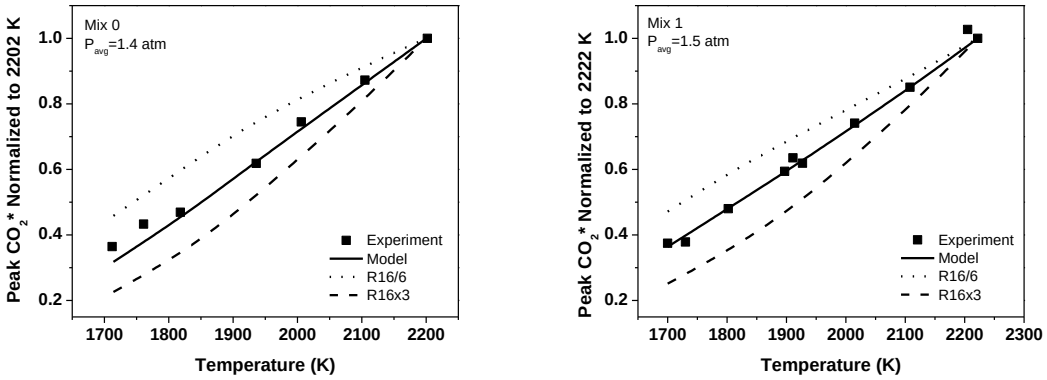

(a) (b)

Figure 11. Effect of changes to $CO + OH \rightleftarrows CO_2 + H$ **(**R16) on mechanism predictions compared to normalized CO_2* peak trends from experiments in Mix 0 (a) and Mix 1 (b).

The upper limit of this rate causes around a 20% under-prediction of peak CO_2* trends in both mixtures, while the lower limit leads to an over-prediction of peak CO_2* by about 25% in Mix 0 and 15% in Mix 1.

Two other minor parameters were also considered in the uncertainty: the effect of the efficiency factors used for R1 and the effect of R2, the CO_2* formation reaction $HCO + O \rightleftharpoons CO_2^* + H$ (see Table 1). Since the sensitivity analyses did not identify R2 as an important reaction for CO_2*, it was of interest to check whether its inclusion in the mechanism made a difference in the final mechanism predictions. Figure 12 shows the effect of omitting the efficiency factors used for R1 and the effect of omitting R2. As expected, these two parameters have little to no effect on the final mechanism predictions.

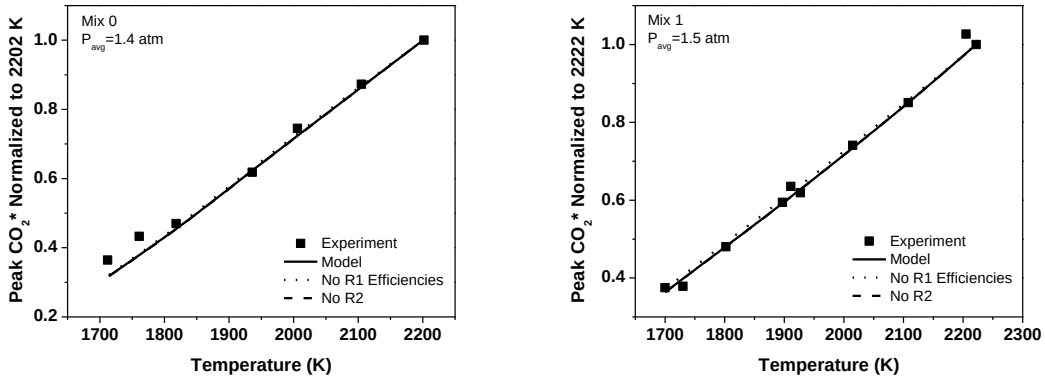

(a) (b)

Figure 12. Effect of omitting the efficiency factors for $CO + O + M \rightleftarrows CO_2^* + M$ (R1) and omitting $HCO + O \rightleftharpoons CO_2^* + H$ (R2) on mechanism predictions compared to normalized CO_2* peak trends from experiments in Mix 0 (a) and Mix 1 (b).

The effect of a combination of the upper and lower bounds of the three most sensitive rates (R3, R15, and R16) would result in about a 35% under-prediction and around a 40% over-prediction of experimental trends in Mix 0. Combining the uncertainties in Mix 1 leads to about a 43% under-prediction and around a 30% over-prediction of experimental trends. These overall uncertainties were calculated by combining the individual uncertainties for each rate in a sum-of-squares fashion.

Comparisons with Past Works

In a previous study at this research facility, CO_2* emission was monitored at 337 nm in a stoichiometric methane-oxygen mixture diluted in 99.1% Ar [9]. Figure 13

shows the CO_2* peak magnitude trends with temperature of that study at an average pressure of 1.3 atm compared with the mechanism predictions of this work. Because this mixture contained CH_4, the mechanism was fortified by the NUIG C4_54.1 chemistry, which can be found at http://c3.nuigalway.ie/mechanisms.html.

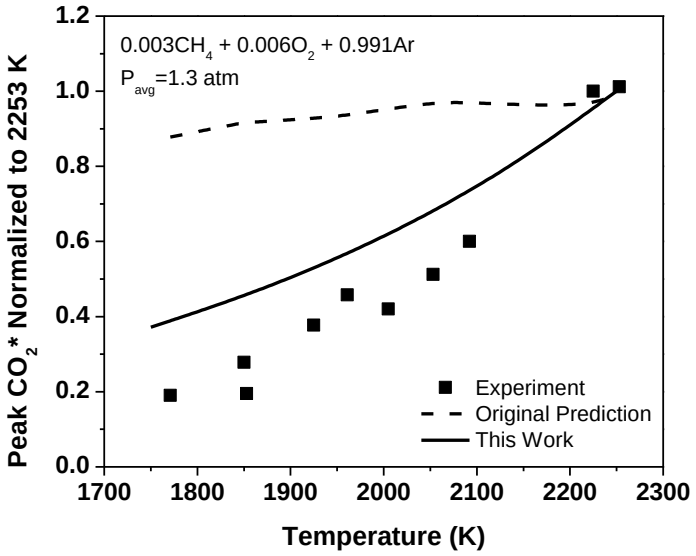

Figure 13. Normalized peak CO_2* from experiments by Petersen et al. [9] in a stoichiometric mixture of methane and oxygen highly diluted in argon at an average pressure of 1.3 atm compared with mechanism predictions from this work.

As the figure shows, there is a slight over-prediction of the data by the model. Although the trend is not completely captured by the mechanism using the rate for R1 determined here, the prediction is far better than what was presented in the original work, shown by the dashed line, which led to over a four-fold over-prediction of the data.

A species time history comparison is presented in Figure 14, which compares an experimental CO_2* profile from [9] to the mechanism predictions from this work at 2092 K and 1.2 atm.

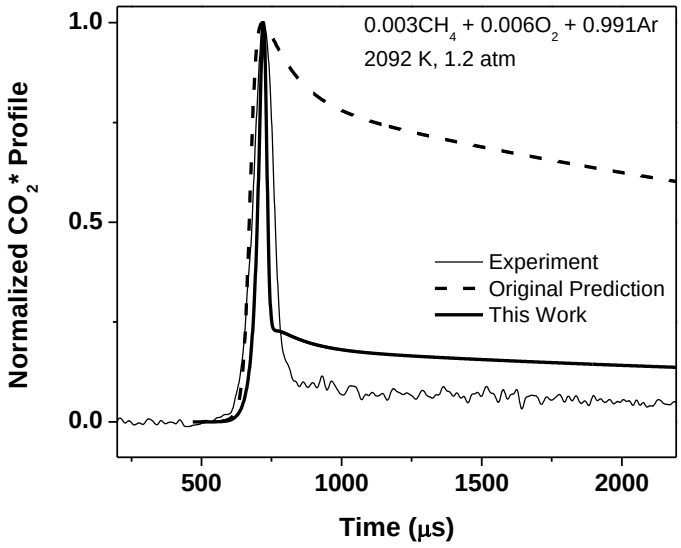

Figure 14. Normalized CO_2* experimental profile at 2092 K and 1.2 atm from [9] compared with the mechanism prediction from this work.

The agreement here is quite good in that the width of the experimental profile is very closely matched with the mechanism prediction. The trailing edge is slightly over-predicted by the mechanism, but this is an extreme improvement over what was presented in the original work, shown by the dashed line, which was around a five-fold over-prediction of the trailing edge. Note that the time history as predicted by the model

was shifted in time to align with the peak of the experimental profile to allow for comparison of the general shape of the profile.

The ability of the mechanism from this work to fairly accurately predict CO_2* peak trends and species time histories in a hydrocarbon mixture adds confidence to the formulations of R1 made herein. It was also of interest to make comparisons with past literature rates of R1. Although only one study has ever quoted a third-order rate for R1 [40], a work by Slack and Grillo [58] formulated a general relationship between CO_2* emission intensity, i_{CO2*}, and the concentration product of [CO] and [O] given by,

$$i_{CO_2^*} = 3.3(\pm 0.3) \times 10^3 \exp(-2{,}300/T)[CO][O]$$

where temperature is in K and concentration units are mole/cm^3. Figure 15 and Figure 16 show the experimental results from this study compared with these two rate expressions alongside the mechanism predictions from this work. As Figure 15 shows, both rate expressions from the literature are quite good at modeling the peak CO_2* trends of the data in both mixtures, although the rate from Sulzmann et al. [40] slightly over-predicts peak trends in Mix 1.

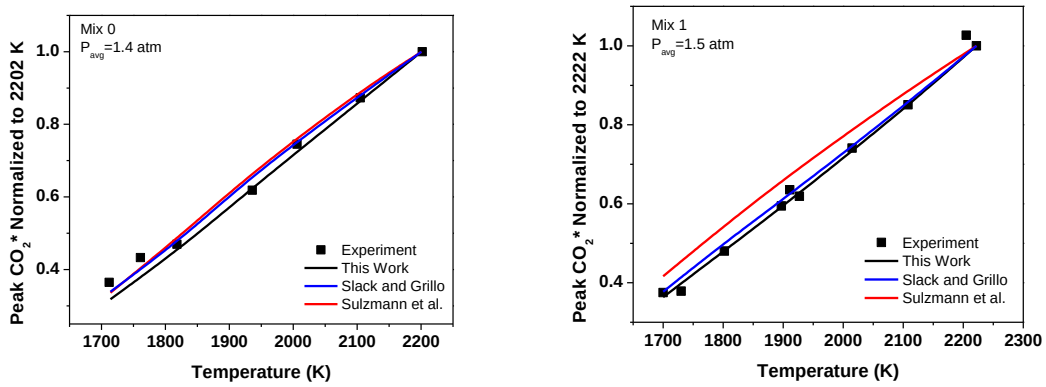

(a) (b)

Figure 15. Normalized peak CO_2* from experiments compared with mechanism predictions from this work, Slack and Grillo [58], and Sulzmann et al. [40] for Mix 0 (a) and Mix 1 (b).

Species time history comparisons are presented in Figure 16 for a moderate temperature in Mix 0 (a) and Mix 1 (b). Time histories from the model predictions were aligned to the rise in CO_2*, rather than the peak, which provided a better visual comparison.

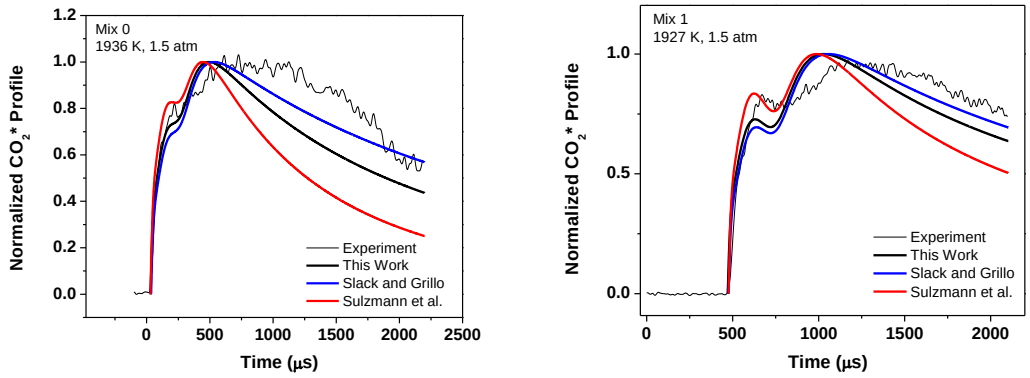

(a) (b)

Figure 16. Normalized CO_2* experimental profiles compared with mechanism predictions from this work, Slack and Grillo [58], and Sulzmann et al. [40] at 1936 K and 1.5 atm in Mix 0 (a) and 1927 K and 1.5 atm in Mix 1 (b).

In Mix 0 (Figure 16 (a)), the leading edge is most closely modeled by the rate for R1 from this work, compared with the other two rate expressions, while the rate expression from Slack and Grillo is the best at modeling the trailing edge of the CO_2* species profile. For Mix 1 (Figure 16 (b)), the trailing edge of the CO_2* profile is again most closely modeled by the rate expression from Slack and Grillo, while the rate from Sulzmann et al. is best at modeling the leading edge. In both cases, the rate for R1 developed in this work falls between the two rate expressions from Slack and Grillo and Sulzmann et al.

Figure 17 shows a typical Arrhenius plot of the natural logarithm of the rate constant for R1 developed in this work compared with that from Sulzmann et al. The

rate for R1 developed by Sulzmann et al. was for a temperature range of 1500 to 3000 K and is as follows:

$$k_{R1} = 2.2 \times 10^{15} \exp\left(-3{,}700/\bar{R}T\right)\ cm^6/mole^2 s$$

where the units for the activation energy are cal/mole. The rate expression from Slack and Grillo could not be included in this plot, as it is only a relation between peak intensity and species concentrations and not a kinetic rate. While the magnitudes of the two rates differ (due to the order of magnitude difference in the pre-exponential factor of both rates), the slopes (indicative of activation energy) are similar, as seen in Figure 17.

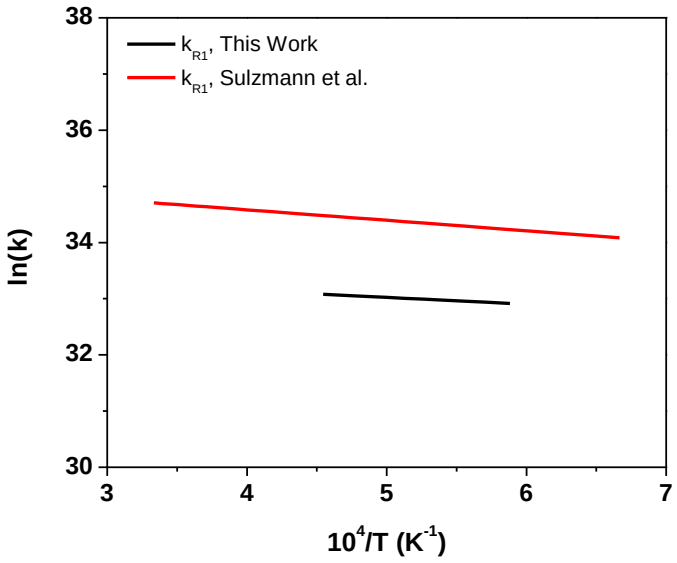

Figure 17. Termolecular rate constants for R1 from Sulzmann et al. and this work plotted against inverse temperature.

High-Pressure Excursion

In the work of Kopp et al. [72], experiments in Mix 0 were also performed at elevated pressures, and it was of interest to compare those results to the model predictions from this work. Figure 18 shows the normalized peak CO_2* trends from the experiments compared with the mechanism developed here.

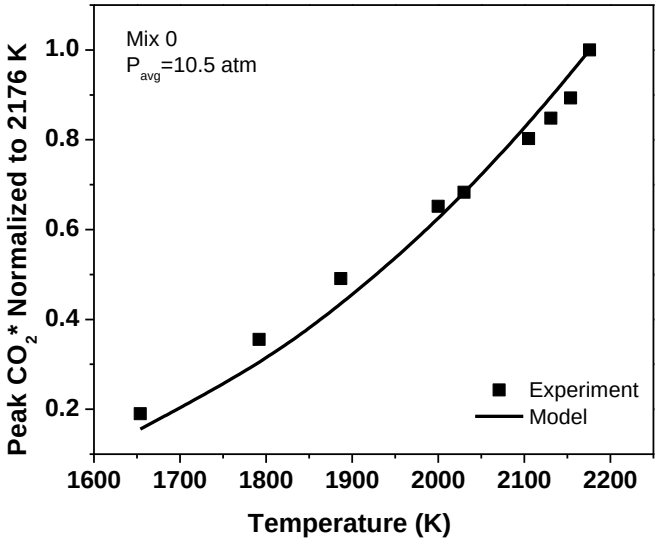

Figure 18. Normalized peak CO_2* from experiments in Mix 0 at an average pressure of 10.5 atm compared with mechanism predictions from this work.

Even though the rate for R1 was calculated using low-pressure data, its ability to predict trends at elevated pressures in Mix 0 is excellent. The experimental CO_2* species time histories are also predicted well by the mechanism, shown in Figure 19. The profiles as

predicted by the model were shifted in time to align with the peak of the experimental profile.

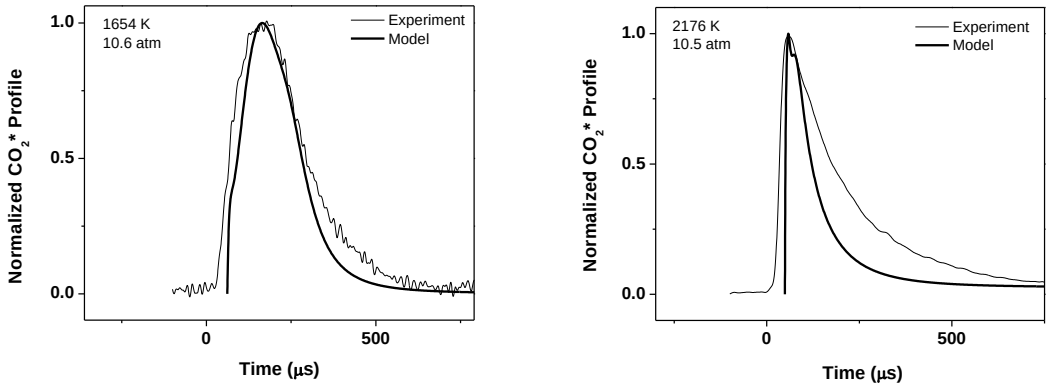

(a) (b)

Figure 19. Normalized CO_2* experimental profiles compared with final mechanism predictions at 1654 K and 10.6 atm (a) and 2176 K and 10.5 atm (b).

For the low-temperature case in Figure 19 (a), the mechanism does an exceptional job at predicting the shape of the CO_2* profile. The agreement between model and experiment slightly lessens as temperature increases, as shown in Figure 19 (b), with the model tending to predict slightly thinner species profiles than the experiment. However, this phenomenon is quite common among high-pressure shock-tube measurements of chemiluminescence species. Overall, the ability of the mechanism to predict high-pressure trends is quite promising.

CHAPTER V

CONCLUSIONS AND RECOMMENDATIONS

CO_2* chemiluminescence measurements were performed in H_2-N_2O-CO-Ar mixtures behind reflected shock waves to evaluate CO_2* chemical kinetics. The experimental results were used to tailor the rate of the main CO_2* formation reaction, CO + O + M $\rightleftarrows$ CO_2* + M (R1). Supporting CO_2* quenching chemistry was determined from basic collision theory. The overall rate expression for R1 was determined as

$$k_{R1} = 4.0 \times 10^{14} \exp\left(-2{,}384/\bar{R}T\right)\ cm^6/mole^2 sec$$

where units of the activation energy are cal/mole. The final mechanism was able to reproduce peak CO_2* trends at both low and elevated pressures in the H_2-N_2O-CO-Ar mixtures. Comparisons with shock-tube data in methane-oxygen mixtures were also made, which showed a slight over-prediction of peak CO_2* experimental trends.

The unique species time histories of CO_2* in the H_2-N_2O-CO-Ar mixtures offered a good test for the mechanism. Although trends were not perfectly matched, the subtleties in the experimental profiles were captured by the mechanism, and slight refinements in some key ground-state reactions could further improve these predictions. Because the rate for R1 could not be completely isolated, its uncertainty was inherently related to the accuracy in a few other reactions, one of which was the quenching of CO_2* by argon. Uncertainty analysis showed that variation in this rate by an order of magnitude caused up to a 30% under- or over-prediction of peak CO_2* trends. Since this rate was determined purely by theoretical calculations, it is recommended that

experiments to validate this rate should be made to add confidence in the value determined for R1.

Now that a full kinetic scheme for CO_2* has been developed, another avenue of research would be to make quantitative measurements of CO_2* by performing a series of low-pressure calibration measurements to correlate PMT output to absolute CO_2* concentration, much like what was done for OH* in the work of Petersen et al. [9]. Coupled with measurements at elevated pressures, this procedure could provide insight into a possible pressure dependence of R1.

REFERENCES

[1] Gupta, S.B., Bihari, B.P., Biruduganti, M.S., Sekar, R.R., Zigan, J., "On Use of CO_2* Chemiluminescence for Combustion Metrics in Natural Gas Fired Reciprocating Engines," *Proceedings of the Combustion Institute*, **33**, 2, (2011), pp. 3131-3139.

[2] Kim, B., Kaneko, M., Ikeda, Y., Nakajima, T., "Detailed Spectral Analysis of the Process of HCCI Combustion," *Proceedings of the Combustion Institute*, **29**, (2002), pp. 671-677.

[3] Najm, H.N., Paul, P.H., Mueller, C.J., Wyckoff, P.S., "On the Adequacy of Certain Experimental Observables as Measurements of Flame Burning Rate," *Combustion and Flame*, **113**, 3, (1998), pp. 312-332.

[4] Samaniego, J.M., Egolfopoulos, F.N., Bowman, C.T., "CO_2* Chemiluminescence in Premixed Flames," *Combustion Science and Technology*, **109**, (1995), pp. 183-203.

[5] Nori, V.N., Seitzman, J.M., "Evaluation of Chemiluminescence as a Combustion Diagnostic under Varying Operating Conditions," *46th AIAA Aerospace Sciences Meeting and Exhibit*, AIAA 2008-953, (2008), pp. 1-14.

[6] Tinaut, F.V., Reyes, M., Giménez, B., Pastor, J.V., "Measurements of OH* and CH* Chemiluminescence in Premixed Flames in a Constant Volume Combustion Bomb under Autoignition Conditions," *Energy & Fuels*, **25**, 1, (2011), pp. 119-129.

[7] Ikeda, Y., Kojima, J., Hashimoto, H., "Local Chemiluminescence Spectra Measurements in a High-Pressure Laminar Methane/Air Premixed Flame," *Proceedings of the Combustion Institute*, **29**, 2, (2002), pp. 1495-1501.

[8] Nori, V.N., Seitzman, J.M., "Chemiluminescence Measurements and Modeling in Syngas, Methane and Jet-A Fueled Combustors," *45th AIAA Aerospace Sciences Meeting and Exhibit*, AIAA-2007-0466, (2007), pp. 1-14.

[9] Petersen, E., Kopp, M., Donato, N., Güthe, F., "Assessment of Current Chemiluminescence Kinetics Models at Engine Conditions," *Journal of Engineering for Gas Turbines and Power*, **134**, 5, (2012), pp. 1-7.

[10] Carrington, T., "Electronic Quenching of OH($^2\Sigma^+$) in Flames and Its Significance in the Interpretation of Rotational Relaxation," *The Journal of Chemical Physics*, **30**, 4, (1959), pp. 1087-1095.

[11] Chan, C.Y., O'Brien, R.J., Hard, T.M., Cook, T.B., "Laser-Excited Fluorescence of the Hydroxyl Radical: Relaxation Coefficients at Atmospheric Pressure," *The Journal of Physical Chemistry*, **87**, (1983), pp. 4966-4974.

[12] Clyne, M.A.A., Holt, P.M., "Reaction Kinetics Involving Ground $X^2\Pi$ and Excited $A^2\Sigma^+$ Hydroxyl Radicals. Part 1. Quenching Kinetics of OH $A^2\Sigma^+$ and Rate Constants for Reactions of OH $X^2\Pi$ with CH_3CCl_3 and CO," *Journal of the Chemical Society, Faraday Transactions 2*, **75**, (1979), pp. 569-581.

[13] Copeland, R.A., Crosley, D.R., "Temperature Dependent Electronic Quenching of OH($A^2\Sigma^+$, ν'=0) Between 230 and 310 K," *The Journal of Chemical Physics*, **84**, 6, (1986), pp. 3099-3105.

[14] Fairchild, P.W., Smith, G.P., Crosley, D.R., "Collisional Quenching of A $^2\Sigma^+$ OH at Elevated Temperatures," *The Journal of Chemical Physics*, **79**, 4, (1983), pp. 1795-1807.

[15] Hidaka, Y., Takahashi, S., Kawano, H., Suga, M., Gardiner, W.C., "Shock-Tube Measurements of the Rate Constant for Excited OH($A^2\Sigma^+$) Formation in the Hydrogen-Oxygen Reaction," *The Journal of Physical Chemistry*, **86**, (1982), pp. 1429-1433.

[16] Jörg, A., Meier, U., Kohse-Höinghaus, K., "Rotational Energy Transfer in OH ($A\ ^2\Sigma^+$, v'=0): A Method for the Direct Determination of State-to-State Transfer Coefficients," *The Journal of Chemical Physics*, **93**, 9, (1990), pp. 6453-6462.

[17] McDermid, I.S., Laudenslager, J.B., "Radiative Lifetimes and Quenching Rate Coefficients for Directly Excited Rotational Levels of OH ($A\ ^2\Sigma^+$,v′=0)," *The Journal of Chemical Physics*, **76**, 4, (1982), pp. 1824-1831.

[18] Morley, C., "The Application of Laser Fluorescence to Detection of Species in Atmospheric Pressure Flames. Relative Quenching Rates of OH by H_2O, H_2, and CO," *Combustion and Flame*, **47**, (1982), pp. 67-81.

[19] Paul, P.H., Durant, J.L.J., Gray, J.A., Furlanetto, M.R., "Collisional Electronic Quenching of OH $A\ ^2\Sigma$ (v'=0) Measured at High Temperature in a Shock Tube," *The Journal of Chemical Physics*, **102**, 21, (1995), pp. 8378-8384.

[20] Selzer, P.M., Wang, C.C., "Quenching Rates and Fluorescence Efficiency in the $A\ ^2\Sigma^+$ State of OH," *The Journal of Chemical Physics*, **71**, 9, (1979), pp. 3786-3791.

[21] Tamura, M., Berg, P.A., Harrington, J.E., Luque, J., Jeffries, J.B., Smith, G.P., Crosley, D.R., "Collisional Quenching of CH(A), OH(A), and NO(A) in Low Pressure Hydrocarbon Flames," *Combustion and Flame*, **114**, (1998), pp. 502-514.

[22] Guyot, D., Güthe, F., Schuermans, B., Lacerelle, A., Paschereit, C.O., "CH*/OH* Chemiluminescence Response of an Atmospheric Premixed Flame Under Varying

Operating Conditions," *Proceedings of the ASME Turbo Expo 2010: Power for Land, Sea and Air*, GT2010-23135, (2010), pp. 1-12.

[23] Haber, L.C., Vandsburger, U., "A Global Reaction Model for OH* Chemiluminescence Applied to a Laminar Flat-Flame Burner," *Combustion Science and Technology*, **175**, 10, (2003), pp. 1859-1891.

[24] Hall, J.M., Petersen, E.L., "An Optimized Kinetics Model for OH Chemiluminescence at High Temperatures and Atmospheric Pressures," *International Journal of Chemical Kinetics*, **38**, (2006), pp. 714-724.

[25] Hall, J.M., Petersen, E.L., "Kinetics of OH Chemiluminescence in the Presence of Hydrocarbons," *40th AIAA/ASME/SAE/ASEE Joint Propulsion Conference & Exhibit*, AIAA 2004-4164, (2004), pp. 1-10.

[26] Higgens, B., McQuay, M.Q., Lacas, F., Rolon, J.C., Darabiha, N., Candel, S., "Systematic Measurements of OH Chemiluminescence for Fuel-lean, High-pressure, Premixed, Laminar Flames," *Fuel*, **80**, (2001), pp. 67-74.

[27] Kathrotia, T., Fikri, M., Bozkurt, M., Hartmann, M., Riedel, U., Schulz, C., "Study of the H + O + M Reaction Forming OH*: Kinetics of OH* Chemiluminescence in Hydrogen Combustion Systems," *Combustion and Flame*, **157**, 7, (2010), pp. 1261-1273.

[28] Garland, N.L., Crosley, D.R., "On the Collisional Quenching of Electronically Excited OH, NH and CH in Flames," *21st International Symposium on Combustion*, (1986), pp. 1693-1702.

[29] Heard, D.E., Jeffries, J.B., Crosley, D.R., "Collisional Quenching of A $^2\Sigma^+$ NO and $A^2\Delta$ CH in Low Pressure Flames," *Chemical Physics Letters*, **178**, 5-6, (1991), pp. 533-537.

[30] Kenner, R.D., Pfannenberg, S., Heinrich, P., Stuhl, F., "Electronic Quenching of CH($A^2\Delta$), NH($A^3\Pi$), CH($c^1\Pi$), and PH($A^3\Pi$) between 240 and 420 K," *The Journal of Physical Chemistry*, **95**, 17, (1991), pp. 6585-6593.

[31] Zhang, R., Crosley, D.R., "Temperature Dependent Quenching of A $^2\Sigma^+$ NO Between 215 and 300 K," *The Journal of Chemical Physics*, **102**, 19, (1995), pp. 7418-7424.

[32] Lauer, M., Sattelmayer, T., "On the Adequacy of Chemiluminescence as a Measure for Heat Release in Turbulent Flames with Mixture Gradients," *Journal of Engineering for Gas Turbines and Power*, **132**, 6, (2010), pp. 1-8.

[33] Mancaruso, E., Vaglieco, B.M., "Spectroscopic Measurements of Premixed Combustion in Diesel Engine," *Fuel*, **90**, 2, (2011), pp. 511-520.

[34] Bessler, W.G., Schulz, C., Lee, T., Jeffries, J.B., Hanson, R.K., "Carbon Dioxide UV Laser-Induced Fluorescence in High-Pressure Flames," *Chemical Physics Letters*, **375**, 3-4, (2003), pp. 344-349.

[35] Clyne, M.A.A., Thrush, B.A., "Mechanism of Chemiluminescent Combination Reactions Involving Oxygen Atoms," *Proceedings of the Royal Society of London. Series A, Mathematical and Physical Sciences*, **269**, 1338, (1962), pp. 404-418.

[36] Davies, W.O., "Carbon Dioxide Dissociation at 6,000 to 11,000 K," *The Journal of Chemical Physics*, **43**, 8, (1965), pp. 2809-2818.

[37] Lee, T., Bessler, W.G., Schulz, C., Patel, M., Jeffries, J.B., Hanson, R.K., "UV Planar Laser Induced Fluorescence Imaging of Hot Carbon Dioxide in a High-Pressure Flame," *Applied Physics B*, **79**, 4, (2004), pp. 427-430.

[38] Schott, G.L., Getzinger, R.W., Seitz, W.A., "Transient Oxygen Atom Yields in H_2-O_2 Ignition and the Rate Coefficient for O + H_2 --> OH + H*," *International Journal of Chemical Kinetics*, **6**, (1974), pp. 921-943.

[39] Smith, G.P., Luque, J., Park, C., Jeffries, J.B., Crosley, D.R., "Low Pressure Flame Determinations of Rate Constants for OH(A) and CH(A) Chemiluminescence," *Combustion and Flame*, **131**, 1-2, (2002), pp. 59-69.

[40] Sulzmann, K.G.P., Myers, B.F., Bartle, E.R., "CO Oxidation. I. Induction Period Preceding CO_2 Formation in Shock-Heated CO-O_2-Ar Mixtures," *The Journal of Chemical Physics*, **42**, 11, (1965), pp. 3969-3979.

[41] Vesel, A., Mozetic, M., Drenik, A., Balat-Pichelin, M., "Dissociation of CO_2 Molecules in Microwave Plasma," *Chemical Physics*, **382**, 1-3, (2011), pp. 127-131.

[42] Gaydon, A.G., *The Spectroscopy of Flames*, Chapman and Hall Ltd, London, 1976.

[43] Kaskan, W.E., "The Source of the Continuum in Carbon Monoxide-Hydrogen-Air Flames," *Combustion and Flame*, **3**, (1959), pp. 39-48.

[44] Ikeda, Y., Kojima, J., Hashimoto, H., Nakajima, T., "Detailed Local Spectra Measurement in High-Pressure Premixed Laminar Flame," *40th Aerospace Sciences Meeting & Exhibit*, AIAA-2002-0191, (2002), pp. 1-8.

[45] Kirby, B.J., Hanson, R.K., "Linear Excitation Schemes for IR Planar-Induced Fluorescence Imaging of CO and CO_2," *Applied Optics*, **41**, 6, (2002), pp. 1190-1201.

[46] Schuermans, B., Güthe, F., Pennell, D., Guyot, D., Paschereit, C.O., "Thermoacoustic Modeling of a Gas Turbine Using Transfer Functions Measured Under Full Engine Pressure," *Journal of Engineering for Gas Turbines and Power*, **132**, 11, (2010), pp. 1-9.

[47] Hall, J.M., de Vries, J., Amadio, A.R., Petersen, E.L., "Towards a Kinetics Model of CH Chemiluminescence," *43rd AIAA Aerospace Sciences Meeting and Exhibit*, AIAA 2005-1318, (2005), pp. 1-11.

[48] Clyne, M.A.A., Thrush, B.A., "The Kinetics of the Carbon Monoxide Flame Bands," *Proceedings of the 9th International Symposium on Combustion*, **9**, 1, (1963), pp. 177-183.

[49] Gordon, A.S., Knipe, R.H., "The Explosive Reaction of Carbon Monoxide and Oxygen at the Second Explosion Limit in Quartz Vessels," *The Journal of Physical Chemistry*, **59**, (1955), pp. 1160-1165.

[50] Lin, M.C., Bauer, S.H., "Bimolecular Reaction of N_2O with CO and the Recombination of O and CO as Studied in a Single-Pulse Shock Tube," *The Journal of Chemical Physics*, **50**, 8, (1969), pp. 3377-3391.

[51] Malerich, C.J., Scanlon, J.H., "Calculation of $CO(X\ ^1\Sigma^+) + O(^3P)$ Recombination Chemiluminescence Spectrum," *Chemical Physics*, **110**, (1986), pp. 303-313.

[52] Myers, B.F., "Shock-Tube Study of the Radiative Processes in Systems Containing Atomic Oxygen and Carbon Monoxide at High Temperature," *The Journal of Chemical Physics*, **47**, 5, (1967), pp. 1783-1792.

[53] Myers, B.F., Sulzmann, K.G.P., Bartle, E.R., "Oxidation of CO. II. Influence of H_2 on the Induction Period Preceding Rapid CO_2 Formation in Shock-Heated CO-O_2-Ar Mixtures," *The Journal of Chemical Physics*, **43**, 4, (1965), pp. 1220-1228.

[54] Pravilov, A.M., Smirnova, L.G., "Temperature Dependence of the Spectral Distribution of the Rate Constant of Chemiluminescence in the Reaction $O(^3P)$ + CO-->CO_2+hv," *Kinetics and Catalysis*, **22**, 4, (1981), pp. 832-838.

[55] Rond, C., Bultel, A., Boubert, P., Chéron, B.G., "Spectroscopic Measurements of Nonequilibrium CO_2 Plasma in RF Torch," *Chemical Physics*, **354**, 1-3, (2008), pp. 16-26.

[56] Schott, G.L., "Further Studies of Exponential Branching Rates in Reflected-Shock Heated, Nonstoichiometric H_2-CO-O_2 Systems," *Combustion and Flame*, **21**, (1973), pp. 357-370.

[57] Simonaitis, R., "Kinetics and Mechanism of the Reaction of $O(^3P)$ with Carbon Monoxide," *The Journal of Chemical Physics*, **56**, 5, (1972), pp. 2004-2011.

[58] Slack, M., Grillo, A., "High Temperature Rate Coefficient Measurements of CO + O Chemiluminescence," *Combustion and Flame*, **59**, (1985), pp. 189-196.

[59] Laidler, K.J., Shuler, K.E., "Elementary Reactions in the Gas Phase Involving Excited Electronic States," *Chemical Reviews*, **48**, 2, (1951), pp. 153-224.

[60] Broida, H.P., Gaydon, A.G., "The Luminous Reaction Between Carbon Monoxide and Atomic Oxygen," *Transactions of the Faraday Society*, **49**, (1953), pp. 1190-1193.

[61] Brokaw, R.S., "Ignition Kinetics of the Carbon Monoxide-Oxygen Reaction," *11th Combustion Symposium*, (1967), pp. 1063-1073.

[62] DeMore, W.B., "Pressure Dependence and Mechanism of the Reaction of Atomic Oxygen and Carbon Monoxide," *The Journal of Physical Chemistry*, **76**, 24, (1972), pp. 3527-3532.

[63] Hartunian, R.A., Thompson, W.P., Hewitt, E.W., "Glow-Discharge Shock Tube for Studying Chemiluminescent, Surface-Catalytic, and Gas-Phase Reaction Rates; Temperature Dependence of NO-O and CO-O Chemiluminescence," *The Journal of Chemical Physics*, **44**, 5, (1966), pp. 1765-1769.

[64] Alwahabi, Z.T., Li, Z.S., Zetterberg, J., Aldén, M., "Infrared Polarization Spectroscopy of CO_2 at Atmospheric Pressure," *Optics Communications*, **233**, 4-6, (2004), pp. 373-381.

[65] Kirby, B.J., Hanson, R.K., "Imaging of CO and CO_2 Using Infrared Planar Laser-Induced Fluorescence," *Proceedings of the Combustion Institute*, **28**, (2000), pp. 253-259.

[66] Roy, S., Lucht, R.P., McIlroy, A., "Mid-Infrared Polarization Spectroscopy of Carbon Dioxide," *Applied Physics B: Lasers and Optics*, **75**, 8, (2002), pp. 875-882.

[67] Zetterberg, J., Blomberg, S., Gustafson, J., Sun, Z.W., Li, Z.S., Lundgren, E., Alden, M., "An *in situ* Set Up for the Detection of CO_2 from Catalytic CO Oxidation by using Planar Laser-Induced Fluorescence," *Review of Scientific Instruments*, **83**, 5, (2012), pp. 1-5.

[68] Jachimowski, C.J., "Kinetics of Oxygen Atom Formation During the Oxidation of Methane Behind Shock Waves," *Combustion and Flame*, **23**, (1974), pp. 233-248.

[69] Toselli, B.M., Barker, J.R., "Excitation of CO_2 by Energy Transfer from Highly Vibrationally Excited Benzene Derivatives," *The Journal of Chemical Physics*, **95**, 11, (1991), pp. 8108-8119.

[70] Dixon, R.N., "The Carbon Monoxide Flame Bands," *Proceedings of the Royal Society of London. Series A, Mathematical and Physical Sciences*, **275**, 1362, (1963), pp. 431-446.

[71] Gardiner, W.C., Mallard, W.G., McFarland, M., Morinaga, K., Owen, J.H., Rawlins, W.T., Takeyama, T., Walker, B.F., "Elementary Reaction Rates from Post-Induction-Period Profiles in Shock-Initiated Combustion," pp. 61-75.

[72] Kopp, M., Brower, M., Mathieu, O., Petersen, E.L., Güthe, F., "CO_2* Chemiluminescence Study at Low and Elevated Pressures," *Applied Physics B*, **107**, (2012), pp. 529-538.

[73] Bowman, C.T., "Non-Equilibrium Radical Concentrations in Shock-Initiated Methane Oxidation," *Fifteenth Symposium (International) on Combustion*, **15**, 1, (1974), pp. 869-882.

[74] Copeland, R.A., Dyer, M.J., Crosley, D.R., "Rotational-Level-Dependent Quenching of $A^2\Sigma^+$ OH and OD," *The Journal of Chemical Physics*, **82**, 9, (1985), pp. 4022-4032.

[75] Turns, S.R., *An Introduction to Combustion: Concepts and Applications*, 2nd ed., McGraw-Hill, 2000.

[76] Aul, C.J., "An Experimental Study into the Ignition of Methane and Ethane Blends in a New Shock-tube Facility," MS Thesis, Mechanical Engineering, Texas A&M University, College Station, TX, 2009.

[77] Petersen, E.L., Rickard, M.J.A., Crofton, M.W., Abbey, E.D., Traum, M.J., Kalitan, D.M., "A Facility for Gas- and Condensed-Phase Measurements Behind Shock Waves," *Measurement Science and Technology*, **16**, 9, (2005), pp. 1716-1729.

[78] CHEMKIN 10112, Reaction Design: San Diego, 2011.

[79] Healy, D., Donato, N.S., Aul, C.J., Petersen, E.L., Zinner, C.M., Bourque, G., Curran, H.J., "Isobutane Ignition Delay Time Measurements at High Pressure and Detailed Chemical Kinetic Simulations," *Combustion and Flame*, **157**, 8, (2010), pp. 1540-1551.

[80] Healy, D., Kopp, M.M., Polley, N.L., Petersen, E.L., Bourque, G., Curran, H.J., "Methane/n-Butane Ignition Delay Measurements at High Pressure and Detailed Chemical Kinetic Simulations," *Energy & Fuels*, **24**, 3, (2010), pp. 1617-1627.

[81] Mathieu, O., Levacque, A., Petersen, E.L., "Effects of N_2O Addition on the Ignition of H_2–O_2 Mixtures: Experimental and Detailed Kinetic Modeling Study," *International Journal of Hydrogen Energy*, **37**, (2012), pp. 15393-15405.

[82] Dean, A.M., Steiner, D.C., Wang, E.E., "A Shock Tube Study of the $H_2/O_2/CO/Ar$ and $H_2/N_2O/CO/Ar$ System: Measurement of the Rate Constant for $H + N_2O = N_2 + OH^*$," *Combustion and Flame*, **32**, (1978), pp. 73-83.

[83] Holtermann, D.L., Lee, E.K.C., Nanes, R., "Rates of Collision-Induced Electronic Relaxation of Single Rotational Levels of SO_2 ($\tilde{A}\ ^1A_2$): Quenching Mechanism by Collision Complex Formation," *The Journal of Chemical Physics*, **77**, 11, (1982), pp. 5327-5339.

[84] Thayer, C.A., Yardley, J.T., "Laser-Excited Electronic Fluorescence: Collision-Induced Radiationless Transitions in Propynal," *The Journal of Chemical Physics*, **57**, 9, (1972), pp. 3992-4001.

[85] Manion, J.A., Huie, R.E., Levin, R.D., Burgess, D.R.Jr., Orkin, V.L., Tsang, W., McGivern, W.S., J. W. Hudgens, Knyazev, V.D., Atkinson, D.B., Chai, E., Tereza, A.M., Lin, C.-Y., T. C. Allison, W. G. Mallard, F. Westley, J. T. Herron, Hampson, R.F., Frizzell, D.H., NIST Chemical Kinetics Database, NIST Standard Reference Database 17, Version 7.0 (Web Version), Release 1.4.3, Data version 2008.12, National Institute of Standards and Technology, Gaithersburg, Maryland, 20899-8320. Web address: http://kinetics.nist.gov/

APPENDIX

Detailed Kinetics Mechanism

```
!AUTHORS:A.K. KEROMNES, W. K. METCALFE, H. J. CURRAN
ELEMENTS
C H N O AR HE
END
SPECIES
H H2 O O2 OH OH*
H2O N2 HO2 H2O2 AR
CO CO2 HE CH4 C2H6 HCO
N       NH      NO      N2O
NH2     N2O3    HNO     NO2     NNH     NH3     N2H2
HONO    NO3     HNO3    N2H3    N2H4    N2O4    NH2OH
HNOH    H2NO    HNNO    CO2(A)
END
REACTIONS
!REF:3 PARAMETER FIT TO HONG ET AL.PROC. OF THE COMB. INST. 33 (2011) 309–
316
H+O2<=>O+OH 9.65E+14 -0.262 1.62E+04
!REF:SUTHERLAND ET AL., 21ST SYMPOSIUM, P. 929 (1986)
O+H2<=>H+OH 5.080E+04 2.670 6.292E+03
!REF:! OLDENBORG,R.C.ET AL. J. PHYS. CHEM. (1992) 96 8426-8430
OH+H2<=>H+H2O 2.247E8 1.520 3.450E+03
!REF:SUTHERLAND ET AL., 23RD SYMPOSIUM, P. 51 (1990) INCREASED BY 16% FOR
H2-CO-H2O FLAMES
O+H2O<=>OH+OH 3.445E+06 2.020 1.340E+04
!REF:TSANG AND HAMPSON, J. PHYS. CHEM. REF. DATA, 15:1087 (1986)
H2+M<=>H+H+M 4.577E+19 -1.400 1.044E+05
H2/ 2.5/ H2O/ 12/ CO/ 1.9/ CO2/ 3.8/ HE/ .83/ CH4/ 2/ C2H6/ 3/
O+O+M<=>O2+M 6.165E+15 -0.500 0.000E+00
H2/ 2.5/ H2O/ 12/ AR/ .83/ CO/ 1.9/ CO2/ 3.8/ HE/ .83/ CH4/ 2/ C2H6/ 3/
O+H+M<=>OH+M 4.714E+18 -1.000 0.000E+00
H2/ 2.5/ H2O/ 12/ AR/ .75/ CO/ 1.5/ CO2/ 2/ HE/ .75/ CH4/ 2/ C2H6/ 3/
!REF: LI IJCK 36: 566–575, 2004
!REF:OPTIMISED TO FIT H2 AND CH4 FLAMES DATA
H+OH+M<=>H2O+M 3.5E+22 -2.000 0.000E+00
H2/ 2.5/ H2O/ 12/ AR/ 0.38/ HE/ 0.38/ CO/ 1.9/ CO2/ 3.8/ CH4/ 2/ C2H6/ 3/
!REF:FERNANDES PCCP 2008
H+O2(+M)<=>HO2(+M) 4.650E+12 0.440 0.000E+00
LOW/ 1.737E+19 -1.23 0.000E+00/
TROE/ 0.67 1E-30 1E30 1E30/
```

H2/ 1.3/ CO/ 1.9/ CO2/ 3.8/ HE/ 0.0/ H2O/ 10.0/ AR/ 0.00/ CH4/ 2/ C2H6/ 3/
H+O2(+AR)<=>HO2(+AR) 4.650E+12 0.440 0.000E+00
!REF: BATES ET AL. PCCP 3 (2001) 2337-2342
LOW/ 6.810E+18 -1.200 0.0/
TROE/ 0.70 1.0E-30 1.0E+30 1.0E+30/
!REF:LPL * 1.5 AK
H+O2(+HE)<=>HO2(+HE) 4.650E+12 0.440 0.000E+00
LOW/ 9.192E+18 -1.20 0.000E+00/
TROE/ 0.59 1E-30 1E30 1E30/
!REF: MUELLER 99
HO2+H<=>OH+OH 7.079E+13 0.00 2.950E+02
!REF:MICHAEL SUTHERLAND 2000
H2+O2<=>H+HO2 5.176E+05 2.433 53502.0
!REF:BAULCH ET AL., J. PHYS. CHEM. REF DATA, 21:411 (1992)
HO2+O<=>OH+O2 3.250E+13 0.000 0.000E+00
!REF:KEYSER, J. PHYS. CHEM. 92:1193 (1988) REDUCED BY 15%
HO2+OH<=>H2O+O2 2.456E+13 0.000 -4.970E+02
!REF:HIPPLER ET AL. J.CHEM.PHYS 93 1755-1760 (1990)
HO2+HO2<=>H2O2+O2 1.300E+11 0.000 -1630.00
DUP
!REF:REDUCED BY 13%
HO2+HO2<=>H2O2+O2 3.658E+14 0.000 12000.00
DUP
!REF:TROE, COMBUST. FLAME, 158:594-601 (2011)
!REF:RATE CONSTANT IS FOR N2
H2O2(+H2O)<=>OH+OH(+H2O) 2.00E+12 0.90 4.8749+04
LOW/ 1.865E+25 -2.30 4.8749+04/
TROE/ 0.51 1E-30 1E+30/
H2O2(+M)<=>OH+OH(+M) 2.00E+12 0.90 4.8749+04
LOW/ 2.49E+24 -2.30 4.8749+04/
TROE/ 0.43 1E-30 1E+30/
H2O/ 0.0/ CO2/ 1.6/ N2/ 1.5/ O2/ 1.2/ HE/ 0.65/ H2O2/ 7.7/
!REF:EFFICIENCIES FOR H2 AND CO TAKEN FROM LI ET AL., INT. J. CHEM. KINET. 36:566-575 (2004)
H2/ 3.7/ CO/ 2.8/
!REF:TSANG AND HAMPSON, J. PHYS. CHEM. REF. DATA, 15:1087 (1986)
H2O2+H<=>H2O+OH 2.410E+13 0.000 3.970E+03
!REF: ELLINGSON J. PHYS. CHEM. (2007) 111, (51), 13554-13566
H2O2+H<=>H2+HO2 2.150E+10 1.000 6.000E+03
!REF:TSANG AND HAMPSON, J. PHYS. CHEM. REF. DATA, 15:1087 (1986)
H2O2+O<=>OH+HO2 9.550E+06 2.000 3.970E+03
!REF: HONG ET AL. J. PHYS. CHEM. A 114 (2010) 5718-5727
H2O2+OH<=>H2O+HO2 1.74E+12 0.000 3.18E+02
DUP
H2O2+OH<=>H2O+HO2 7.59E+13 0.000 7.269E+03
DUP
!REF:MEULLER 99 * 0.76
CO+O(+M)<=>CO2(+M) 1.362E+10 0.000 2384.00

```
LOW/ 1.173E+24 -2.79 4191.0/
H2/ 2.0/ H2O/ 12/ CO/ 1.75/ CO2/ 3.6/ AR/ 0.7/ HE/ 0.7/
!REF:86TSA/ HAM * 0.44
CO+O2<=>CO2+O 1.119E+12 0.000 47700.00
!REF: JOSHI AND WANG IJCK (2006), 38, (1), 57-73.
CO+OH<=>CO2+H 7.015E+04 2.053 -355.67
DUP
CO+OH<=>CO2+H 5.757E+12 -0.664 331.83
DUP
!REF:YOU ET AL. J. PHYS. CHEM. A 2007, 111, 4031-4042
CO+HO2<=>CO2+OH 1.570E+05 2.180 1.794E+04
!REF:LI ET AL. IJCK 2007
HCO+M<=>H+CO+M 4.750E+11 0.660 1.487E+04
H2/ 2/ H2O/ 12/ CO/ 1.5/ CO2/ 2/ CH4/ 2/ C2H6/ 3/
!REF:TIMONEN ET AL., JPC, 92:651 (1988)
HCO+O2<=>CO+HO2 7.580E+12 0.000 4.100E+02
HCO+H<=>CO+H2 7.340E+13 0.000 0.000E+00
!REF:TSANG AND HAMPSON, J. PHYS. CHEM. REF. DATA, 15:1087 (1986)
HCO+O<=>CO+OH 3.020E+13 0.000 0.000E+00
HCO+O<=>CO2+H 3.000E+13 0.000 0.000E+00
!REF:TIMONEN ET AL., JPC, 92:651 (1988)
HCO+OH<=>CO+H2O 1.020E+14 0.000 0.000E+00
!REF:TSANG AND HAMPSON, J. PHYS. CHEM. REF. DATA, 15:1087 (1986)
HCO+HO2=>CO2+H+OH 3.000E+13 0.000 0.000E+00
!REF:TSANG AND HAMPSON, J. PHYS. CHEM. REF. DATA, 15:1087 (1986)
HCO+HCO=>H2+CO+CO 3.000E+12 0.000 0.000E+00
!§§§§§§§§§§§§§§§§§§§§§§§§§§§§§§§§§§§§§§§§§§§§§§§§§§§§§§§§§§§§§§§§§§§§
!§§§§§§§§§§§§§§§§§§§§§§   NOX REACTIONS   §§§§§§§§§§§§§§§§§§§§§§§§§
!§§§§§§§§§§§§§§§§§§§§§§§§§§§§§§§§§§§§§§§§§§§§§§§§§§§§§§§§§§§§§§§§§§§§
! NO REACTIONS
N2+O=>NO+N          1.80E+14   0.00     76100    ! 41    KONNOV
NO+N=>N2+O          2.11E+13   0.00         0    ! 42    BAULCH
N+O2=NO+O           9.00E+09   1.00      6500    ! 43    KONNOV
NO+M=N+O+M          9.64E+14   0.00    148300    ! 44    KONNOV
N2 /1.5/ NO /3.0/
NO+NO=N2+O2         3.00E+11   0.00     65000    ! 45    KONNOV
NO+O(+M)=NO2(+M)    1.30E+15  -0.75         0    ! 46    KONNOV
LOW /4.72E+24 -2.87 1551/
TROE /0.962 10.0 7962/
AR /0.6/ NO2 /6.2/ NO /1.8/ O2 /0.8/ N2O /4.4/ H2O /10.0/
HO2+NO=NO2+OH       2.11E+12   0.00      -479    ! 47    HOWARD, J. AM.
CHEM. SOC., 102, 6937, 1980. (SUGG. BY TSANG)
N+OH=NO+H           2.00E+13   0.00         0    ! 48    MICK AND ROTH, J. PHYS.
CHEM. 98 (1994) 5310-5313.
! NO2 REACTIONS
NO2+O=NO+O2         3.91E+12   0.00      -238    ! 49    KONNOV
NO2+N=N2O+O         8.40E+11   0.00         0    ! 50    KONNOV
NO2+N=NO+NO         1.00E+12   0.00         0    ! 51    KONNOV
```

```
NO2+NO=N2O+O2                1.00E+12   0.00      60000       ! 52       KONNOV
NO2+NO2=NO+NO+O2              3.95E+12   0.00      27590       ! 53       KONNOV
NO2+NO2=NO3+NO               1.13E+04   2.58      22720       ! 54       KONNOV
NO2+O(+M)=NO3(+M)             1.33E+13   0.00         0       ! 55       KONNOV
LOW /1.49E+28 -4.08 2467/
TROE /0.86 10.0 2800/
H2O/10.0/ O2/0.8/ H2/2.0/
NO2+NO(+M)=N2O3(+M)           1.60E+09   1.40         0       ! 56       KONNOV
    LOW /1.0E+33  -7.7  0.0/
    N2/1.36/
NO2+H2=HONO+H                 7.33E+11   0.00      28810       ! 57       MODIFIED RATE
FROM TSANG&HERRON WITH OUR H2/NO2 AND H2/O2/NOX EXPERIMENTS
NO2+H=NO+OH                  1.32E+14   0.00        362       ! 58       KO,T. AND
FONTIJN,A.,J.PHYS.CHEM.,95,3984,1991.
! N2O REACTIONS
N2O(+M)=N2+O(+M)              9.9E+10   0.00      57960       ! 59A      BAULCH
   LOW /6.62E+14 0 57500/                                    ! 59B      BAULCH 6.62E+14 CORRECT
   O2/1.4/ N2/1.7/ H2O/12.0/ NO/3.0/ N2O/3.5/                !          KONNOV
N2O+O=N2+O2                  3.69E+12   0.00      15944       ! 60       MEAGHER J. PHYS.
CHEM. A, 2000, 104(25), P 6003.
N2O+O=NO+NO                   9.15E+13   0.00      27693       ! 61       MEAGHER J. PHYS.
CHEM. A, 2000, 104(25), P 6003.
N2O+N=N2+NO                  1.00E+13   0.00      20000       ! 62       KONNOV
N2O+NO=N2+NO2                 2.75E+14   0.00      50000       ! 63       KONNOV
N2O+H=N2+OH                  3.31E+10   0.00       5090       ! 64       BAULCH
DUP
N2O+H=N2+OH                  7.83E+14   0.00      19390       ! 65       BAULCH
DUP
!N2O+H=N2+OH                  2.58E-26   4.39       1455       ! 64       DIAU
N2O+OH=HO2+N2                       2.00E+12   0.00      40000       ! 66       MEV
! NO3 REACTIONS
NO3=NO+O2                   2.50E+06   0.00      12120       ! 67       KONNOV
NO3+NO2=NO+NO2+O2             1.20E+11   0.00       3200       ! 68       KONNOV
NO3+O=NO2+O2                 1.02E+13   0.00          0       ! 69       KONNOV
NO3+NO3=NO2+NO2+O2            5.12E+11   0.00       4870       ! 70       KONNOV
! N2O4 REACTIONS
N2O4(+M)=NO2+NO2(+M)          4.05E+18  -1.10      12840       ! 71       KONNOV
    LOW /1.96E+28  -3.8  12840./
    AR/0.8/ N2O4/2.0/ NO2/2.0/
N2O4+O=N2O3+O2               1.21E+12   0.00          0       ! 72       KONNOV
! N2O3 REACTIONS
N2O3+O=NO2+NO2                2.71E+11   0.00          0       ! 73       KONNOV
! N2 REACTIONS
N2+M=N+N+M                   1.00E+28  -3.33     225000       ! 74       KONNOV
   N/5/ O/2.2/
! HONO REACTIONS
N2O4+H2O=HONO+HNO3            2.52E+14   0.00      11590       ! 75       KONNOV
N2O3+H2O=HONO+HONO            3.79E+13   0.00       8880       ! 76       KONNOV
```

```
NO+OH(+M)=HONO(+M)              2.00E+12  -0.05       -721       ! 77       KONNOV
   LOW / 5.08E+23 -2.51 -67.6 /
   TROE /0.62 10.0 100000.0 /
   H2O/10.0/ O2/2.0/ AR/0.75/ H2/2.0/
NO2+H+M=HONO+M                  1.40E+18  -1.50       900       ! 78       KONNOV
HONO+H=HNO+OH                   5.64E+10   0.86      4970       ! 79       KONNOV
HONO+H=NO+H2O                   8.12E+06   1.89      3840       ! 80       KONNOV
HONO+O=OH+NO2                   1.20E+13   0.00      5960       ! 81       KONNOV
HONO+OH=H2O+NO2                 1.69E+12   0.00      -517       ! 82       KONNOV
HONO+NH=NH2+NO2                 1.00E+13   0.00         0       ! 83       KONNOV
HONO+HONO=H2O+NO2+NO            1.00E+13   0.00      8540       ! 84       KONNOV
HONO+NH2=NO2+NH3                5.00E+12   0.00         0       ! 85       KONNOV
! HNO REACTIONS
HNO+NO=N2O+OH                   8.50E+12   0.00     29580       ! 86       KONNOV
HNO+NO+NO=HNNO+NO2              1.60E+11   0.00      2090       ! 87       KONNOV
H+NO(+M)=HNO(+M)                1.52E+15  -0.41         0       ! 88       KONNOV
   LOW /4.00E+20 -1.75 0.0 /
   H2O/10.0/ O2/1.5/ AR/0.75/ H2/2.0/
HNO+H=NO+H2                     4.46E+11   0.72       655       ! 89       KONNOV
HNO+OH=NO+H2O                   1.30E+07   1.88      -956       ! 90       KONNOV
HNO+O=OH+NO                     5.00E+11   0.50      2000       ! 91       KONNOV
HNO+O=NO2+H                     5.00E+10   0.00      2000       ! 92       KONNOV
HNO+O2=NO+HO2                   2.20E+10   0.00      9140       ! 93       KONNOV
HNO+N=NO+NH                     1.00E+11   0.50      2000       ! 94       KONNOV
HNO+N=H+N2O                     5.00E+10   0.50      3000       ! 95       KONNOV
HNO+NH2=NH3+NO                  2.00E+13   0.00      1000       ! 96       KONNOV
HNO+HNO=N2O+H2O                 3.63E-03   3.98      1190       ! 97       KONNOV
HNO+HNO=HNOH+NO                 2.00E+08   0.00      4170       ! 98       KONNOV
HNO+NO2=HONO+NO                 6.02E+11   0.00      2000       ! 99       KONNOV
! HNO3 REACTIONS
NO2+OH(+M)=HNO3(+M)             2.41E+13   0.00         0       !100       KONNOV
   LOW / 6.42E+32 -5.49 2350.0 /
   TROE /1.0 10.0 1168.0 /
   H2O/10.0/ O2/2.0/ AR/0.75/ H2/2.0/
NO+HO2+M=HNO3+M                 1.50E+24  -3.50      2200       !101       KONNOV
HNO3+H=H2+NO3                   5.56E+08   1.53     16400       !102       KONNOV
HNO3+H=H2O+NO2                  6.08E+01   3.29      6290       !103       KONNOV
HNO3+H=OH+HONO                  3.82E+05   2.30      6980       !104       KONNOV
HNO3+OH=NO3+H2O                 1.03E+10   0.00     -1240       !105       KONNOV
! HNNO REACTIONS
NH+NO+M=HNNO+M                  1.63E+23  -2.60      1820       !106       KONNOV
HNNO+H=N2O+H2                   2.00E+13   0.00         0       !107       KONNOV
HNNO+H=NH2+NO                   1.00E+12   0.00         0       !108       KONNOV
HNNO+O=N2O+OH                   2.00E+13   0.00         0       !109       KONNOV
HNNO+OH=H2O+N2O                 2.00E+13   0.00         0       !110       KONNOV
HNNO+OH=HNOH+NO                 1.00E+12   0.00         0       !111       KONNOV
HNNO+NO=N2+HONO                 2.60E+11   0.00      1610       !112       KONNOV
HNNO+NO=NNH+NO2                 3.20E+12   0.00       540       !113       KONNOV
```

```
HNNO+NO=N2O+HNO                 1.00E+12   0.00         0       !114       KONNOV
HNNO+NO2=N2O+HONO               1.00E+12   0.00         0       !115       KONNOV
HNNO+NO2=NNH+NO3                1.00E+13   0.00     17000       !116       KONNOV
! H2NO REACTIONS
H2NO+M=H2+NO+M                  7.83E+27  -4.29     60300       !117       KONNOV
  H2O/10.0/
H2NO+M=HNO+H+M                  2.80E+24  -2.83     64915       !118       KONNOV
  H2O/10.0/
H2NO+M=HNOH+M                   1.10E+29  -3.99     43980       !119       KONNOV
  H2O/10.0/
H2NO+H=HNO+H2                   3.00E+07   2.00      2000       !120       KONNOV
H2NO+H=NH2+OH                   5.00E+13   0.00         0       !121       KONNOV
H2NO+O=HNO+OH                   3.00E+07   2.00      2000       !122       KONNOV
H2NO+OH=HNO+H2O                 2.00E+07   2.00      1000       !123       KONNOV
H2NO+HO2=HNO+H2O2               2.90E+04   2.69     -1600       !124       KONNOV
H2NO+NH2=HNO+NH3                3.00E+12   0.00      1000       !125       KONNOV
H2NO+O2=HNO+HO2                 3.00E+12   0.00     25000       !126       KONNOV
H2NO+NO=HNO+HNO                 2.00E+07   2.00     13000       !127       KONNOV
H2NO+NO2=HONO+HNO               6.00E+11   0.00      2000       !128       KONNOV
! HNOH REACTIONS
HNOH+M=HNO+H+M                  2.00E+24  -2.84     58935       !129       KONNOV
   H2O/10.0/
HNOH+H=HNO+H2                   4.80E+08   1.50       380       !130       KONNOV
HNOH+H=NH2+OH                   4.00E+13   0.00         0       !131       KONNOV
HNOH+O=HNO+OH                   7.00E+13   0.00         0       !132       KONNOV
    DUPLICATE
HNOH+O=HNO+OH                   3.30E+08   1.50      -360       !133       KONNOV
    DUPLICATE
HNOH+OH=HNO+H2O                 2.40E+06   2.00     -1190       !134       KONNOV
HNOH+HO2=HNO+H2O2               2.90E+04   2.69     -1600       !135       KONNOV
HNOH+NH2=HNO+NH3                1.80E+06   1.94     -1150       !136       KONNOV
HNOH+NO2=HONO+HNO               6.00E+11   0.00      2000       !137       KONNOV
HNOH+O2=HNO+HO2                 3.00E+12   0.00     25000       !138       KONNOV
HNOH+HNO=NH2OH+NO               1.00E+12   0.00      3000       !139       KONNOV
! NH2OH REACTIONS
NH2OH+OH=HNOH+H2O               2.50E+13   0.00      4250       !140       KONNOV
!§§§§§§§§§§§§§§§§§§§§§§§§§§§§§§§§§§§§§§§§§§§§§§§§§§§§§§§§§§§§§§§§§§
!§§§§§§§§§§§§§§§§§§§§§   NXHY REACTIONS   §§§§§§§§§§§§§§§§§§§§§§§§
!§§§§§§§§§§§§§§§§§§§§§§§§§§§§§§§§§§§§§§§§§§§§§§§§§§§§§§§§§§§§§§§§§§
! NH REACTIONS FROM ALLEN ET AL. COMB. FLAME  109, 449 (1997)
NH+O2=HNO+O                     3.89E+13   0.00     17890       !141
MERTENS,J.D.,CHANG,HANSON,&BOWMAN,IJCK,23,173,1991
NH+O2=NO+OH                     7.60E+10   0.00      1530       !142
MERTENS,J.D.,CHANG,HANSON,&BOWMAN,IJCK,23,173,1991
NH+O=NO+H                       5.50E+13   0.00         0       !143
MERTENS,CHANG,HANSON,&BOWMAN,IJCK,23,173,1991
NH+OH=HNO+H                     2.00E+13   0.00         0       !144
MILLER&BOWMAN,PROG.ENERGYCOMBUST.SCI.,15,287,1989.
```

NH+NO=N2O+H 3.13E+14 -0.45 0 !145 MILLER AND MELIUS, 24TH INT.SYMP.COMB.,1992 (REFITTÉ POUR FORMAT CTI (A NÉGATIF))
NH+NO=N2+OH 2.16E+13 -0.23 0 !146 MILLER AND MELIUS, 24TH INT.SYMP.COMB.,1992
NH+NO2=NO+HNO 1.00E+11 0.50 4000 !147 CFM
NH+NH=N2+H+H 5.10E+13 0.00 0 !148 MERTENS,CHANG,HANSON,&BOWMAN,IJCK,21,1049,1989.
! NH2 REACTIONS FROM ALLEN ET AL. COMB. FLAME 109, 449 (1997)
NH2+O=HNO+H 6.63E+14 -0.50 0 !149 MILLER&BOWMAN,PROG.ENERGYCOMBUST.SCI.,15,287,1989.
NH2+O=NH+OH 6.75E+12 0.00 0 !150 MILLER&BOWMAN,PROG.ENERGYCOMBUST.SCI.,15,287,1989.
H+NH2=H2+NH 7.20E+05 2.32 1587 !151 LINDER...PAGE, J. PHYS. CHEM., 99, 11458, 1995 APPARENTLY AGREES WITH ROEHRIG'S DATA
NH2+OH=NH+H2O 4.00E+06 2.00 1000 !152 LIN, WANG, LIN, MELIUS, INT. J. CHEM. KINET., 22, 454, 1990.
NH2+NO=NNH+OH 2.80E+13 -0.55 0 !153 GLARBORG'S DENOX MECHANISM
NH2+NO=N2+H2O 5.16E+17 -1.82 0 !154 GLARBORG'S DENOX MECHANISM (REFITTÉ POUR FORMAT CTI (A NÉGATIF))
NH2+NO=N2O+H2 5.00E+13 0.00 24640 !155 CFM
NH2+NO=HNO+NH 1.00E+13 0.00 4000 !156 CFM
NH2+NO2=N2O+H2O 3.28E+18 -2.20 0 !157 MILLER & BOWMAN, INT. J. CHEM. KINET., 23, 289, 1991.
NH2+NH2=NH3+NH 5.00E+13 0.00 10000 !158 GLARBORG ET AL., INT. J. CHEM. KINET., 26, 421, 1994.
NH+NH2=N2H2+H 3.16E+13 0.00 994 !159 HANSON
NH2+NH2=N2H2+H2 3.98E+13 0.00 11922 !160 HANSON
! NH3 REACTIONS FROM ALLEN ET AL. COMB. FLAME 109, 449 (1997)
NH3+M=NH2+H+M 2.20E+16 0.00 93470 !161 GLARBORG ET AL., INT. J. CHEM. KINET., 26, 421, 1994.
NH2+HO2=NH3+O2 1.00E+13 0.00 0 !162 GLARBORG ET AL., INT. J. CHEM. KINET., 26, 421, 1994.
NH2+O2=HNO+OH 1.78E+12 0.00 14900 !163 HANSON & SALIMIAN, IN COMBUSTION CHEMISTRY, GARDINER, ED., SPRINGER-VERLAG, 1984.
NH3+O=NH2+OH 9.40E+06 1.94 6460 !164 GLARBORG ET AL., INT. J. CHEM. KINET., 26, 421, 1994.
NH3+H=NH2+H2 6.40E+05 2.39 10170 !165 GLARBORG ET AL., INT. J. CHEM. KINET., 26, 421, 1994.
NH3+OH=NH2+H2O 2.04E+06 2.04 566 !166 MILLER&BOWMAN,PROG.ENERGYCOMBUST.SCI.,15,287,1989.
NH3+HO2=NH2+H2O2 3.00E+11 0.00 22000 !167 GLARBORG ET AL., INT. J. CHEM. KINET., 26, 421, 1994.
NH3+NH2=N2H3+H2 7.94E+11 0.50 21559 !168 HANSON
! NNH REACTIONS FROM ALLEN ET AL. COMB. FLAME 109, 449 (1997)
NNH+M=N2+H+M 1.00E+14 0.00 3000 !169 DIAU, YU, WAGNER, LIN, J.PHYS. CHEM. 98, 4034, 1994.

NNH+H=N2+H2 1.00E+14 0.00 0 !170 GLARBORG ET AL., INT. J. CHEM. KINET., 26, 421, 1994.
NNH+OH=N2+H2O 5.00E+13 0.00 0 !171 GLARBORG ET AL., INT. J. CHEM. KINET., 26, 421, 1994.
NNH+NO=N2+HNO 5.00E+13 0.00 0 !172 MILLER&BOWMAN,PROG.ENERGYCOMBUST.SCI.,15,287,1989.
NNH+NH=N2+NH2 5.00E+13 0.00 0 !173 GLARBORG ET AL., INT. J. CHEM. KINET., 26, 421, 1994.
NNH+NH2=N2+NH3 5.00E+13 0.00 0 !174 GLARBORG ET AL., INT. J. CHEM. KINET., 26, 421, 1994.
NNH+NNH=N2H2+N2 1.00E+13 0.00 9935 !175 HANSON
! N2H2 REACTIONS FROM ALLEN ET AL. COMB. FLAME 109, 449 (1997)
N2H2+H=NNH+H2 1.00E+13 0.00 994 !176 HANSON
N2H2+NH=NNH+NH2 1.00E+13 0.00 994 !177 HANSON
N2H2+M=NNH+H+M 1.00E+16 0.00 49675 !178 HANSON
N2H2+M=NH+NH+M 3.16E+16 0.00 99350 !179 HANSON
N2H2+NH2=NNH+NH3 1.00E+13 0.00 3974 !180 HANSON
N2H2+NH2=NH+N2H3 1.00E+11 0.50 33779 !181 HANSON
N2H2+N2H2=NNH+N2H3 1.00E+13 0.00 9935 !182 HANSON
N2H2+O=NNH+OH 1.00E+11 0.50 0 !183 HANSON
N2H2+OH=NNH+H2O 1.00E+13 0.00 1987 !184 HANSON
N2H2+HO2=NNH+H2O2 1.00E+13 0.00 1987 !185 HANSON
! N2H3 REACTIONS FROM ALLEN ET AL. COMB. FLAME 109, 449 (1997)
N2H3+H=N2H2+H2 1.00E+12 0.00 1987 !186 HANSON
N2H3+H=NH2+NH2 1.58E+12 0.00 0 !187 HANSON
N2H3+H=NH+NH3 1.00E+11 0.00 0 !188 HANSON
N2H3+NH2=N2H2+NH3 1.00E+11 0.50 0 !189 HANSON
N2H3+M=N2H2+H+M 1.00E+16 0.00 49675 !190 HANSON
N2H3+M=NH2+NH+M 1.00E+16 0.00 41727 !191 HANSON
N2H3+N2H2=N2H4+NNH 1.00E+13 0.00 9935 !192 HANSON
N2H3+O=N2H2+OH 3.16E+11 0.50 0 !193 HANSON
N2H3+O=NNH+H2O 3.16E+11 0.50 0 !194 HANSON
N2H3+OH=N2H2+H2O 1.00E+13 0.00 1987 !195 HANSON
N2H3+HO2=N2H2+H2O2 1.00E+13 0.00 1987 !196 HANSON
! N2H4 REACTIONS FROM ALLEN ET AL. COMB. FLAME 109, 449 (1997)
N2H4+NH2=N2H3+NH3 3.98E+11 0.50 1987 !197 HANSON
N2H4+H=N2H3+H2 1.29E+13 0.00 2503 !198 HANSON
N2H4+H=NH2+NH3 4.46E+09 0.00 3099 !199 HANSON
N2H4+M=NH2+NH2+M 4.00E+15 0.00 40932 !200 HANSON
N2H4+M=N2H3+H+M 1.00E+15 0.00 63584 !201 HANSON
N2H4+N2H2=N2H3+N2H3 2.50E+10 0.50 29805 !202 HANSON
N2H4+O=N2H2+H2O 6.31E+13 0.00 1192 !203 HANSON
N2H4+O=N2H3+OH 2.51E+12 0.00 1192 !204 HANSON
N2H4+OH=N2H3+H2O 3.98E+13 0.00 0 !205 HANSON
N2H4+HO2=N2H3+H2O2 3.98E+13 0.00 1987 !206 HANSON
NH+NO=O+NNH 1.85E+13 0.21 9931 ! DEAN AND BOZZELI

!Begin OH* model**********

```
H+O+M=OH*+M                    3.100E+14 0.0     10000
OH*+AR=OH+AR                    2.170E+10      0.5      2060
OH*+H2O=OH+H2O                   5.920E+12      0.5   -8.61E2
OH*+CO2=OH+CO2                   2.750E+12      0.5   -9.68E2
OH*+CO=OH+CO                    3.230E+12      0.5   -7.87E2
OH*+H2=OH+H2                    2.950E+12      0.5   -4.44E2
OH*+O2=OH+O2                    2.100E+12      0.5   -4.82E2
OH*+OH=OH+OH                     1.500E+12      0.5       0.0
OH*+H=OH+H                     1.500E+12      0.5       0.0
OH*+O=OH+O                     1.500E+12      0.5       0.0
OH*+CH4=OH+CH4                   3.360E+12      0.5   -6.35E2
OH*+N2=OH+N2                                1.080E+11       0.5   -1238.0
OH*=OH+HV                    1.400E+06      0.0       0.0
N2O+H=OH*+N2                1.60E+14   0.00      50300       ! 30       Hidaka J. phy. chem., 89,
4903
!End OH* model*********************************************************

!CO2* Mechanism
CO+O+M<=>CO2(A)+M 4.0E+14 0.000 2.384E+03
H2/2.0/ H2O/12/ CO/1.75/ CO2/3.6/ AR/0.7/ HE/0.7/
HCO+O<=>CO2(A)+H 3.000E+13 0.000 0.000E+00
!CO2* Quenching
CO2(A)+AR<=>CO2+AR                 8.421E+12      0.5      0.0
CO2(A)+H2O<=>CO2+H2O               8.339E+12      0.5      0.0
CO2(A)+CO2<=>CO2+CO2               9.115E+12      0.5      0.0
CO2(A)+CO<=>CO2+CO                 9.687E+12      0.5      0.0
CO2(A)+H<=>CO2+H                   3.065E+13      0.5      0.0
CO2(A)+H2<=>CO2+H2                 2.2710E+13     0.5      0.0
CO2(A)+O2<=>CO2+O2                 8.774E+12      0.5      0.0
CO2(A)+O<=>CO2+O                  9.819E+12      0.5      0.0
CO2(A)+OH<=>CO2+OH                 9.872E+12      0.5      0.0
CO2(A)+CH4<=>CO2+CH4               1.190E+13      0.5      0.0
CO2(A)+N2<=>CO2+N2                 9.963e12         0.5      0.0
CO2(A)<=>CO2+HV                    1.000E+06      0.0      0.0

END
```

Thermodynamic Data

```
!AUTHORS:A.K. KEROMNES, W. K. METCALFE, H. J. CURRAN
THERMO
   300.000  1000.000  5000.000
H               L 6/94H   1    0    0    0G   200.000  6000.00  1000.00      1
 0.25000000E+01 0.00000000E+00 0.00000000E+00 0.00000000E+00 0.00000000E+00    2
```

0.25473660E+05-0.44668285E+00 0.25000000E+01 0.00000000E+00 0.00000000E+00 3
0.00000000E+00 0.00000000E+00 0.25473660E+05-0.44668285E+00 0.26219035E+05 4
H2 TPIS78H 2 0 0 0G 200.000 6000.00 1000.00 1
2.93286575E+00 8.26608026E-04-1.46402364E-07 1.54100414E-11-6.88804800E-16 2
-8.13065581E+02-1.02432865E+00 2.34433112E+00 7.98052075E-03-1.94781510E-05 3
2.01572094E-08-7.37611761E-12-9.17935173E+02 6.83010238E-01 0.00000000E+00 4
O L 1/90O 1 0 0 0G 200.000 6000.00 1000.00 1
2.54363697E+00-2.73162486E-05-4.19029520E-09 4.95481845E-12-4.79553694E-16 2
2.92260120E+04 4.92229457E+00 3.16826710E+00-3.27931884E-03 6.64306396E-06 3
-6.12806624E-09 2.11265971E-12 2.91222592E+04 2.05193346E+00 2.99687009E+04 4
O2 RUS 89O 2 0 0 0G 200.000 6000.00 1000.00 1
3.66096065E+00 6.56365811E-04-1.41149627E-07 2.05797935E-11-1.29913436E-15 2
-1.21597718E+03 3.41536279E+00 3.78245636E+00-2.99673416E-03 9.84730201E-06 3
-9.68129509E-09 3.24372837E-12-1.06394356E+03 3.65767573E+00 0.00000000E+00 4
OH IU3/03O 1 H 1 0 0G 200.000 6000.00 1000.00 1
2.83853033E+00 1.10741289E-03-2.94000209E-07 4.20698729E-11-2.42289890E-15 2
3.69780808E+03 5.84494652E+00 3.99198424E+00-2.40106655E-03 4.61664033E-06 3
-3.87916306E-09 1.36319502E-12 3.36889836E+03-1.03998477E-01 4.48613328E+03 4
OH* 121286O 1H 1 G 0300.00 5000.00 1000.00 1
0.02882730E+02 0.10139743E-02-0.02276877E-05 0.02174683E-09-0.05126305E-14 2
5.02650000E+04 0.05595712E+02 0.03637266E+02 0.01850910E-02-0.16761646E-05 3
0.02387202E-07-0.08431442E-11 5.00213000E+04 0.13588605E+01 4
H2O L 5/89H 2 O 1 0 0G 200.000 6000.00 1000.00 1
0.26770389E+01 0.29731816E-02-0.77376889E-06 0.94433514E-10-0.42689991E-14 2
-0.29885894E+05 0.68825500E+01 0.41986352E+01-0.20364017E-02 0.65203416E-05 3
-0.54879269E-08 0.17719680E-11-0.30293726E+05-0.84900901E+00-0.29084817E+05 4
N2 G 8/02N 2 0 0 0G 200.000 6000.00 1000.00 1
2.95257637E+00 1.39690040E-03-4.92631603E-07 7.86010195E-11-4.60755204E-15 2
-9.23948688E+02 5.87188762E+00 3.53100528E+00-1.23660988E-04-5.02999433E-07 3
2.43530612E-09-1.40881235E-12-1.04697628E+03 2.96747038E+00 0.00000000E+00 4
HO2 T 1/09H 1O 2 0 0G 200.000 5000.00 1000.00 1
4.17228741E+00 1.88117627E-03-3.46277286E-07 1.94657549E-11 1.76256905E-16 2
3.10206839E+01 2.95767672E+00 4.30179807E+00-4.74912097E-03 2.11582905E-05 3
-2.42763914E-08 9.29225225E-12 2.64018485E+02 3.71666220E+00 1.47886045E+03 4
H2O2 T 8/03H 2O 2 0 0G 200.000 6000.00 1000.00 1
4.57977305E+00 4.05326003E-03-1.29844730E-06 1.98211400E-10-1.13968792E-14 2
-1.80071775E+04 6.64970694E-01 4.31515149E+00-8.47390622E-04 1.76404323E-05 3
-2.26762944E-08 9.08950158E-12-1.77067437E+04 3.27373319E+00-1.63425145E+04 4
AR G 5/97AR 1 0 0 0G 200.000 6000.00 1000.00 1
2.50000000E+00 0.00000000E+00 0.00000000E+00 0.00000000E+00 0.00000000E+00 2
-7.45375000E+02 4.37967491E+00 2.50000000E+00 0.00000000E+00 0.00000000E+00 3
0.00000000E+00 0.00000000E+00-7.45375000E+02 4.37967491E+00 0.00000000E+00 4
CO RUS 79C 1O 1 0 0G 200.000 6000.00 1000.00 1
0.30484859E+01 0.13517281E-02-0.48579405E-06 0.78853644E-10-0.46980746E-14 2
-0.14266117E+05 0.60170977E+01 0.35795335E+01-0.61035369E-03 0.10168143E-05 3
0.90700586E-09-0.90442449E-12-0.14344086E+05 0.35084093E+01-0.13293628E+05 4
CO2 L 7/88C 1O 2 0 0G 200.000 6000.00 1000.00 1
0.46365111E+01 0.27414569E-02-0.99589759E-06 0.16038666E-09-0.91619857E-14 2

-0.49024904E+05-0.19348955E+01 0.23568130E+01 0.89841299E-02-0.71220632E-05 3
0.24573008E-08-0.14288548E-12-0.48371971E+05 0.99009035E+01-0.47328105E+05 4
HE G 5/97HE 1 0 0 0 G 200.000 6000.00 1000.00 1
2.50000000E+00 0.00000000E+00 0.00000000E+00 0.00000000E+00 0.00000000E+00 2
-7.45375000E+02 9.28723974E-01 2.50000000E+00 0.00000000E+00 0.00000000E+00 3
0.00000000E+00 0.00000000E+00-7.45375000E+02 9.28723974E-01 0.00000000E+00 4
CH4 G 8/99C 1 H 4 0 0 G 200.000 6000.00 1000.00 1
1.65326226E+00 1.00263099E-02-3.31661238E-06 5.36483138E-10-3.14696758E-14 2
-1.00095936E+04 9.90506283E+00 5.14911468E+00-1.36622009E-02 4.91453921E-05 3
-4.84246767E-08 1.66603441E-11-1.02465983E+04-4.63848842E+00-8.97226656E+03 4
C2H6 G 8/88C 2H 6 0 0G 200.000 6000.00 1000.00 1
4.04666411E+00 1.53538802E-02-5.47039485E-06 8.77826544E-10-5.23167531E-14 2
-1.24473499E+04-9.68698313E-01 4.29142572E+00-5.50154901E-03 5.99438458E-05 3
-7.08466469E-08 2.68685836E-11-1.15222056E+04 2.66678994E+00-1.00849652E+04 4
HCO T 5/03C 1 H 1 O 1 0 G 200.000 6000.00 1000.00 1
3.92001542E+00 2.52279324E-03-6.71004164E-07 1.05615948E-10-7.43798261E-15 2
3.65342928E+03 3.58077056E+00 4.23754610E+00-3.32075257E-03 1.40030264E-05 3
-1.34239995E-08 4.37416208E-12 3.87241185E+03 3.30834869E+00 5.08749163E+03 4
HNNO 103190H 1N 2O 1 G 0300.00 4000.00 1500.00 1
0.06991217E+02 0.01875970E-01-0.02124584E-05-0.06710472E-09 0.12305080E-13 2
0.02497566E+06-0.11235229E+02 0.02238298E+02 0.13591997E-01-0.11798728E-04 3
0.05392970E-07-0.10108589E-11 0.02660258E+06 0.14136789E+02 4
H2NO 102290H 2N 1O 1 G 0300.00 4000.00 1500.00 1
0.05673346E+02 0.02298836E-01-0.01774445E-05-0.11034818E-09 0.01859762E-12 2
0.05569325E+05-0.06153540E+02 0.02530589E+02 0.08596035E-01-0.05471030E-04 3
0.02276249E-07-0.04648073E-11 0.06868030E+05 0.11266506E+02 4
HNOH 102290H 2N 1O 1 G 0300.00 4000.00 1500.00 1
0.06396134E+02 0.01821067E-01-0.01870891E-05-0.07844471E-09 0.14448555E-13 2
0.07859615E+05-0.10404785E+02 0.02125274E+02 0.10662818E-01-0.07602588E-04 3
0.03081641E-07-0.05726498E-11 0.09553544E+05 0.13096718E+02 4
NH2OH WRA032798 N 1H 3O 1 0G 200.000 6000.000 1000.0 1
3.98241375E+00 7.99825642E-03-2.74883544E-06 4.22874218E-10-2.42498273E-14 2
-6.44279418E+03 3.22666600E+00 2.67285464E+00 1.13645347E-02-4.92179546E-06 3
-9.18041765E-11 6.06669407E-13-6.08956846E+03 1.00068112E+01-4.83091791E+00 4
N L 6/88N 1 0 0 0G 200.000 6000.00 1000.0 1
0.24159429E+01 0.17489065E-03-0.11902369E-06 0.30226244E-10-0.20360983E-14 2
0.56133775E+05 0.46496095E+01 0.25000000E+01 0.00000000E+00 0.00000000E+00 3
0.00000000E+00 0.00000000E+00 0.56104638E+05 0.41939088E+01 0.56850013E+05 4
N2O4 RUS 89N 2O 4 0 0G 200.000 6000.000 1000.0 1
1.15752899E+01 4.01616086E-03-1.57178323E-06 2.68274309E-10-1.66922019E-14 2
-2.92191226E+03-3.19488439E+01 3.02002308E+00 2.95904321E-02-3.01342458E-05 3
1.42360407E-08-2.44100049E-12-6.40040162E+02 1.18059606E+01 1.33632866E+03 4
N2O3 L 4/90N 2O 3 0 0G 200.000 6000.000 1000.0 1
9.08583845E+00 3.37756330E-03-1.31583890E-06 2.30762329E-10-1.47151267E-14 2
7.27160146E+03-1.55361904E+01 5.81083964E+00 1.43330962E-02-1.96208597E-05 3
1.73060735E-08-6.46553954E-12 8.19184453E+03 1.20461321E+00 1.04192062E+04 4
NO 121286N 1O 1 G 0300.00 5000.00 1000.00 1
0.03245435E+02 0.01269138E-01-0.05015890E-05 0.09169283E-09-0.06275419E-13 2

0.09800840E+05 0.06417294E+02 0.03376542E+02 0.01253063E-01-0.03302751E-04 3
0.05217810E-07-0.02446263E-10 0.09817961E+05 0.05829590E+02 4
NO2 121286N 1O 2 G 0300.00 5000.00 1000.00 1
0.04682859E+02 0.02462429E-01-0.01042259E-04 0.01976902E-08-0.01391717E-12 2
0.02261292E+05 0.09885985E+01 0.02670600E+02 0.07838501E-01-0.08063865E-04 3
0.06161715E-07-0.02320150E-10 0.02896291E+05 0.01161207E+03 4
HNO 121286H 1N 1O 1 G 0300.00 5000.00 1000.00 1
0.03615144E+02 0.03212486E-01-0.01260337E-04 0.02267298E-08-0.01536236E-12 2
0.01066191E+06 0.04810264E+02 0.02784403E+02 0.06609646E-01-0.09300223E-04 3
0.09437980E-07-0.03753146E-10 0.01091878E+06 0.09035629E+02 4
HONO 31787H 1N 1O 2 G 0300.00 5000.00 1000.00 1
0.05486893E+02 0.04218065E-01-0.01649143E-04 0.02971877E-08-0.02021148E-12 2
-0.01126865E+06-0.02997002E+02 0.02290413E+02 0.01409922E+00-0.01367872E-03 3
0.07498780E-07-0.01876905E-10-0.01043195E+06 0.01328077E+03 4
N2O 121286N 2O 1 G 0300.00 5000.00 1000.00 1
0.04718977E+02 0.02873714E-01-0.01197496E-04 0.02250552E-08-0.01575337E-12 2
0.08165811E+05-0.01657250E+02 0.02543058E+02 0.09492193E-01-0.09792775E-04 3
0.06263845E-07-0.01901826E-10 0.08765100E+05 0.09511222E+02 4
NO3 121286N 1O 3 G 0300.00 5000.00 1000.00 1
0.07120307E+02 0.03246228E-01-0.01431613E-04 0.02797053E-08-0.02013008E-12 2
0.05864479E+05-0.01213730E+03 0.01221076E+02 0.01878797E+00-0.01344321E-03 3
0.01274601E-07 0.01354060E-10 0.07473144E+05 0.01840203E+03 4
HNO3 121286H 1N 1O 3 G 0300.00 5000.00 1000.00 1
0.07003845E+02 0.05811493E-01-0.02333789E-04 0.04288814E-08-0.02959385E-12 2
-0.01889952E+06-0.01047863E+03 0.01353185E+02 0.02220025E+00-0.01978812E-03 3
0.08773908E-07-0.01658384E-10-0.01738563E+06 0.01851868E+03 4
NH 31387H 1N 1 G 0300.00 5000.00 1000.00 1
0.02760249E+02 0.01375346E-01-0.04451914E-05 0.07692792E-09-0.05017592E-13 2
0.04207828E+06 0.05857199E+02 0.03339758E+02 0.01253009E-01-0.03491646E-04 3
0.04218812E-07-0.01557618E-10 0.04185047E+06 0.02507181E+02 4
NH2 121686N 1H 2 G 0300.00 5000.00 1000.00 1
0.02961311E+02 0.02932699E-01-0.09063600E-05 0.01617257E-08-0.01204200E-12 2
0.02191977E+06 0.05777878E+02 0.03432493E+02 0.03299540E-01-0.06613600E-04 3
0.08590947E-07-0.03572047E-10 0.02177228E+06 0.03090111E+02 4
NH3 121386N 1H 3 G 0300.00 5000.00 1000.00 1
0.02461904E+02 0.06059166E-01-0.02004977E-04 0.03136003E-08-0.01938317E-12 2
-0.06493270E+05 0.07472097E+02 0.02204352E+02 0.01011476E+00-0.01465265E-03 3
0.01447235E-06-0.05328509E-10-0.06525488E+05 0.08127138E+02 4
NNH 120186N 2H 1 G 0250.00 4000.00 1000.00 1
0.04415342E+02 0.01614388E-01-0.01632894E-05-0.08559846E-09 0.01614791E-12 2
0.02788029E+06 0.09042888E+01 0.03501344E+02 0.02053587E-01 0.07170410E-05 3
0.04921348E-08-0.09671170E-11 0.02833347E+06 0.06391837E+02 4
N2H2 121286N 2H 2 G 0300.00 5000.00 1000.00 1
0.03371185E+02 0.06039968E-01-0.02303854E-04 0.04062789E-08-0.02713144E-12 2
0.02418172E+06 0.04980585E+02 0.01617999E+02 0.01306312E+00-0.01715712E-03 3
0.01605608E-06-0.06093639E-10 0.02467526E+06 0.01379467E+03 4
N2H3 120186N 2H 3 G 0300.00 5000.00 1000.00 1
0.04441846E+02 0.07214271E-01-0.02495684E-04 0.03920565E-08-0.02298950E-12 2

0.01664221E+06-0.04275205E+01 0.03174204E+02 0.04715907E-01 0.01334867E-03 3
-0.01919685E-06 0.07487564E-10 0.01727270E+06 0.07557224E+02 4
N2H4 121286N 2H 4 G 0300.00 5000.00 1000.00 1
0.04977317E+02 0.09595519E-01-0.03547639E-04 0.06124299E-08-0.04029795E-12 2
0.09341219E+05-0.02962990E+02 0.06442606E+00 0.02749730E+00-0.02899451E-03 3
0.01745240E-06-0.04422282E-10 0.01045192E+06 0.02127789E+03 4
CO2(A) L 7/88C 1O 2 0 0G 200.000 6000.00 1000.00 1
0.46365111E+01 0.27414569E-02-0.99589759E-06 0.16038666E-09-0.91619857E-14 2
-1.03030400E+03-0.19348955E+01 0.23568130E+01 0.89841299E-02-0.71220632E-05 3
0.24573008E-08-0.14288548E-12-3.73971000E+02 0.99009035E+01-0.47328105E+05 4
END